ARL 63-75

HIGH SPEED LOW DENSITY FLOW NEAR THE STAGNATION POINT OF A BLUNT BODY

REUBEN RU-REN CHOW

POLYTECHNIC INSTITUTE OF BROOKLYN
BROOKLYN, NEW YORK

MAY 1963

AERONAUTICAL RESEARCH LABORATORIES
OFFICE OF AEROSPACE RESEARCH
UNITED STATES AIR FORCE

NOTICES

When Government drawings, specifications, or other data are used for any purpose other than in connection with a definitely related Government procurement operation, the United States Government thereby incurs no responsibility nor any obligation whatsoever; and the fact that the Government may have formulated, furnished, or in any way supplied the said drawings, specifications, or other data, is not to be regarded by implication or otherwise as in any manner licensing the holder or any other person or corporation, or conveying any rights or permission to manufacture, use, or sell any patented invention that may in any way be related thereto.

- - - - - - - - - -

Qualified requesters may obtain copies of this report from the Armed Services Technical Information Agency, (ASTIA), Arlington Hall Station, Arlington 12, Virginia.

- - - - - - - - - -

This report has been released to the Office of Technical Services, U. S. Department of Commerce, Washington 25, D. C. for sale to the general public.

- - - - - - - - - -

Copies of ARL Technical Documentary Reports should not be returned to Aeronautical Research Laboratory unless return is required by security considerations, contractual obligations, or notices on a specific document.

33-832, 300, 6-24-63

Aeronautical Research Laboratories, Wright-Patterson AFB, O. HIGH SPEED LOW DENSITY FLOW NEAR THE STAGNATION POINT OF A BLUNT BODY by Rueben Ru-ren Chow, PIB, Brooklyn, N. Y. May 1963. 49 p. incl. illus. (Project 7064; Task 7064-01) (Contract AF 33(616)-7661) (ARL 63075)

Unclassified Report

The analysis is concerned with the investigation of the flow field near the stagnation point of a blunt body in a high speed low density stream. The leading order shock conditions are obtained from the systematic order of magnitude analysis. A matching scheme for the components of heat flux and stresses between the shock and the

(over)

UNCLASSIFIED

1. Hypersonic Aerodynamics
2. Heat Transfer
3. Low Density Flow

I. Reuben Ru-ren Chow
II. Aeronautical Research Laboratories
III. Contract AF 33(616)-7661

UNCLASSIFIED

Aeronautical Research Laboratories, Wright-Patterson AFB, O. HIGH SPEED LOW DENSITY FLOW NEAR THE STAGNATION POINT OF A BLUNT BODY by Rueben Ru-ren Chow, PIB, Brooklyn, N. Y. May 1963. 49 p. incl. illus. (Project 7064; Task 7064-01) (Contract AF 33(616)-7661) (ARL 63075)

Unclassified Report

The analysis is concerned with the investigation of the flow field near the stagnation point of a blunt body in a high speed low density stream. The leading order shock conditions are obtained from the systematic order of magnitude analysis. A matching scheme for the components of heat flux and stresses between the shock and the

(over)

UNCLASSIFIED

1. Hypersonic Aerodynamics
2. Heat Transfer
3. Low Density Flow

I. Reuben Ru-ren Chow
II. Aeronautical Research Laboratories
III. Contract AF 33(616)-7661

UNCLASSIFIED

boundary layer has been proposed for the flow field study. A method of solution has been introduced so that the laborious job of numerical integration of the flow equations with complicated boundary conditions can be bypassed. Calculation has been performed for M_∞=5.7 and T_0=free stream stagnation temperature = 2100°R. Numerical results are presented for the surface heat transfer value, the matching distance, the density and the stagnation enthalpy at the matching surface as functions of the Reynolds number.

UNCLASSIFIED

UNCLASSIFIED

boundary layer has been proposed for the flow field study. A method of solution has been introduced so that the laborious job of numerical integration of the flow equations with complicated boundary conditions can be bypassed. Calculation has been performed for M_∞=5.7 and T_0=free stream stagnation temperature = 2100°R. Numerical results are presented for the surface heat transfer value, the matching distance, the density and the stagnation enthalpy at the matching surface as functions of the Reynolds number.

UNCLASSIFIED

Aeronautical Research Laboratories, Wright-Patterson AFB, O. HIGH SPEED LOW DENSITY FLOW NEAR THE STAGNATION POINT OF A BLUNT BODY by Rueben Ru-ren Chow, PIB, Brooklyn, N. Y. May 1963. 49 p. incl. illus. (Project 7064;Task 7064-01) (Contract AF 33(616)-7661) (ARL 63075)

Unclassified Report

The analysis is concerned with the investigation of the flow field near the stagnation point of a blunt body in a high speed low density stream. The leading order shock conditions are obtained from the systematic order of magnitude analysis. A matching scheme for the components of heat flux and stresses between the shock and the boundary layer has been proposed for the flow field study. A method of solution has been introduced so that the laborious job of numerical integration of the flow equations with complicated boundary conditions can be bypassed. Calculation has been performed for M_∞=5.7 and T_0=free stream stagnation temperature = 2100°R. Numerical results are presented for the surface heat transfer value, the matching distance, the density and the stagnation enthalpy at the matching surface as functions of the Reynolds number.

(over)

UNCLASSIFIED

1. Hypersonic Aerodynamics
2. Heat Transfer
3. Low Density Flow

I. Reuben Ru-ren Chow
II. Aeronautical Research Laboratories
III. Contract AF 33(616)-7661

UNCLASSIFIED

Aeronautical Research Laboratories, Wright-Patterson AFB, O. HIGH SPEED LOW DENSITY FLOW NEAR THE STAGNATION POINT OF A BLUNT BODY by Rueben Ru-ren Chow, PIB, Brooklyn, N. Y. May 1963. 49 p. incl. illus. (Project 7064;Task 7064-01) (Contract AF 33(616)-7661) (ARL 63075)

Unclassified Report

The analysis is concerned with the investigation of the flow field near the stagnation point of a blunt body in a high speed low density stream. The leading order shock conditions are obtained from the systematic order of magnitude analysis. A matching scheme for the components of heat flux and stresses between the shock and the boundary layer has been proposed for the flow field study. A method of solution has been introduced so that the laborious job of numerical integration of the flow equations with complicated boundary conditions can be bypassed. Calculation has been performed for M_∞=5.7 and T_0=free stream stagnation temperature = 2100°R. Numerical results are presented for the surface heat transfer value, the matching distance, the density and the stagnation enthalpy at the matching surface as functions of the Reynolds number.

(over)

UNCLASSIFIED

1. Hypersonic Aerodynamics
2. Heat Transfer
3. Low Density Flow

I. Reuben Ru-ren Chow
II. Aeronautical Research Laboratories
III. Contract AF 33(616)-7661

UNCLASSIFIED

ARL 63-75

HIGH SPEED LOW DENSITY FLOW NEAR THE STAGNATION POINT OF A BLUNT BODY

REUBEN RU-REN CHOW

POLYTECHNIC INSTITUTE OF BROOKLYN
BROOKLYN, NEW YORK

MAY 1963

CONTRACT AF 33(616)-7661
PROJECT 7064
TASK 7064-01

AERONAUTICAL RESEARCH LABORATORIES
OFFICE OF AEROSPACE RESEARCH
UNITED STATES AIR FORCE
WRIGHT-PATTERSON AIR FORCE BASE, OHIO

FOREWORD

This interim report was prepared by Mr. Reuben Ru-ren Chow, Research Fellow, and presents research carried out under Contract No. AF 33(616)-7661, "Research on Thermal and Aerodynamic Effects at Hypersonic Mach Numbers in High Speed Flow," Project No. 7064, "Aerothermodynamic Investigations in High Speed Flow," Task No. 7064-01, "Research on Hypersonic Flow Phenomena." This contract is administered by the Aeronautical Research Laboratories, Office of Aerospace Research, United States Air Force, and is partially supported by the Ballistic Systems Division. Colonel Andrew Boreske, Jr. of the Hypersonic Research Laboratory, ARL, is the contract monitor.

The author wishes to express his sincere gratitude to Professors Antonio Ferri and Lu Ting for their supervision and encouragement during the preparation of this report.

ABSTRACT

The boundary layer thickness around a blunt-nosed body increases as the Reynolds number decreases. When this thickness reaches a magnitude of the order of the inviscid shock detachment distance, the heat fluxes and the components of stresses after the shock begin to play important roles in the flow field behind the shock. These effects necessitate the modification of the usual Rankine-Hugoniot shock conditions in the study of the energy transfer between the fluid and the body surface.

In the present analysis the leading order shock conditions are obtained from the systematic order of magnitude analysis. A complete matching scheme for the components of heat flux and stresses between the shock and the boundary layer is proposed for the study of the flow field as well as the surface heat transfer to the body. No postulation, except the axial symmetry, has been made concerning the shape of the shock. The shape of the matching surface can be obtained uniquely from the present analysis. A method of solution has been introduced so that the laborious job of numerical integration of the flow equations with complicated boundary conditions can be bypassed. The governing equations are transformed and reduced to algebraic forms with the knowledge of the usual similarity solutions of the boundary layer equations.

Calculation has been performed for the specific case of $M_\infty = 5.7$ and T_o = the free stream stagnation temperature = 2100°R. The heat transfer result at the stagnation point is in good agreement with the experimental value and shows a slight improvement to Cheng's Thin Shock Layer Theory in the range of application of the present schemes. The density and the stagnation enthalpy at the matching point are obtained as functions of the Reynolds number. They both show the appropriate asymptotic values of a discontinuous shock as the Reynolds number increases. The matching distance and the shock eccentricity are also obtained as functions of the Reynolds number.

TABLE OF CONTENTS

LIST OF ILLUSTRATIONS

LIST OF TABLES

LIST OF SYMBOLS

Physical Quantities

h	specific enthalpy
h_s	stagnation enthalpy
p	pressure
T	temperature
u	circumferential component of velocity in the meridian plane of a spherical coordinate system
U	free stream velocity
v	radial component of velocity in the meridian plane of a spherical coordinate system
ρ	density

Coordinates

e	$= \frac{\overline{O_B O_s}}{R_B}$ = eccentricity of the shock
r	radial coordinate in the meridian plane of a spherical coordinate system
(r_B, θ_B)	refers to body-centered coordinate system
(r_B, θ_s)	referes to shock-centered coordinate system
R_B	body radius on the axis of symmetry
R_s	shock radius on the axis of symmetry
y	$= \frac{r_B - R_B}{R_B}$
y_1	refers to y at the shock
(η, ξ)	boundary layer coordinates
θ	circumferential coordinate in the meridian plane of a spherical coordinate system

LIST OF SYMBOLS (Contd)

Coefficients of the Transport Properties

k	the coefficient of heat conduction
P_r	Prandtl number
ϵ	$= \frac{\mu_\infty}{\rho_\infty U R_B}$
μ	the shear coefficient of viscosity
μ'	the bulk coefficient of viscosity
ν	$= \frac{\mu_\infty}{\rho_\infty U R_s}$
Γ	$= (\frac{c_p}{c_v})$
$\overline{\varphi}$	$= \frac{\varphi}{\varphi_\infty}$, φ stands for any physical quantity
subscript ∞	refers to the free stream value

SECTION I

INTRODUCTION

At high Reynolds number, the problem of hypersonic cold blunt body heat transfer is considered to be solved within the framework of the boundary layer analysis with negligible boundary layer thickness[1,2]. The thin boundary layer near the wall remains to be a good approximation to the flow field around the body. Consistent with the cold wall and the hypersonic assumptions, similarity solution of the boundary layer equations can be obtained with the usual classical boundary conditions. As the free stream density decreases, this model no longer provides an adequate picture of the flow field around the body, and it is necessary to study the errors imbedded in the scheme.

The effect of the vorticity interaction and its importance to the flow characteristics around the body has been first pointed out by Ferri and Libby[3]. The shock generated vorticity in the inviscid flow behind the shock is a function of the detachment distance, and increases with an increase of free stream velocity. On the other hand, the average shearing stress in the boundary layer decreases as a result of increasing in the boundary layer thickness. When the shearing stresses in the boundary layer and the inviscid shear layer outside become comparable to each other, the interference effect which exists between the two layers becomes important to the flow field behind the shock. Investigation has been made on this effect, and theory has been developed in reference 4 on the heat transfer of a blunt hypersonic geometric configuration as a function of parameters characterizing the vorticity and the boundary layer thickness after the shock. The theory is based on a postulation that for a cold blunt body the boundary layer displacement effect is negligibly small as compared with the effect of the vorticity interaction. With a boundary layer-inviscid shear layer-discontinuous shock model,

---

Manuscript released February 28, 1963 by the author for publication as as ARL Technical Documentary Report.

the boundary layer solution has been obtained by matching both the velocity and the shear with the inviscid layer at a point determined by matching the mass flow. The experimental data on heat transfer value[5] show that the theory is verified down to the range of Reynolds number based on the quantities after the shock of the order of 500 or more. At this range of Reynolds number, an estimation shows that the boundary layer thickness is almost of the order of the inviscid detachment distance. The theory breaks down beyond this point where the stress components and the components of the heat flux after the shock begin to play an important role in the flow field around the body[6].

Van Dyke[7] has made the general discussion on the second order effects, such as the curvature effect, the velocity slip and temperature jump effects at the wall, the vorticity effect and the displacement effect due to the first order boundary layer. Using the usual inner-outer two layer expansion scheme, the first order and the second order equations are presented with boundary conditions obtained by using the standard asymptotic matching technique. The second order effects are expressed in terms of the first and the second order solutions. In the formulation of the problem, the outer layer as defined in reference 7 has been treated without considering the existence of the shock wave. This implies that the range of Reynolds number which the theory is to apply has to be high to ensure the convergence of such an expansion scheme. The boundary layer thickness is much smaller than the inviscid detachment distance. At this range of Reynolds number, the effect of the displacement thickness may be of the same degree of importance as the effect of the vorticity interaction. It is known that to obtain the first order boundary layer solution requires the knowledge of the first order inviscid solution, while the second order boundary layer solution requires the knowledge of the next order solution in the outer layer. This theoretically speaking, can be obtained only by solving the boundary value problem between the perturbed body and the perturbed shock, if the displacement effect is to be considered consistently. In the application to the blunt body problem in reference 7, numerical results have been presented for all the second order effects except, the displacement

effect, due to the extreme complication involved. No new scheme has been proposed concerning this matter. The effects of velocity slip and temperature jump reported in reference 7 have been questioned by Cheng in a recent review[15], since these effects cannot be important insomuch as the problem of cold blunt body in hypersonic flow is considered.

Probstein[8] has proposed the classification of the "flow regimes" according to the degree of rarefiedness of the surrounding flow field of a blunt body reentering the atmosphere with hypersonic speed. In a comprehensive review concerning the subject[9], these flow regimes are discussed in a manner that shows the general picture of the development of the shock wave and of the flow field as the free stream density decreases. No rigorous treatment has been presented concerning the ranges of applications of these regimes, therefore they cannot be regarded as a conclusive statement on the subject. In fact, the existence of the "Viscous Layer Regime" defined by Probstein has been questioned by several authors[7]. Different schemes have been proposed for the solutions in the "Vorticity Interaction Regime," the "Viscous Layer Regime," and the "Incipient Merged Layer Regime"[8,10,11] as defined by Probstein. In reference 10, Probstein and Kemp have adopted the constant density model in treating the flow in the "Viscous Layer Regime." Such a model, as pointed out by Cheng[15], describes more appropriately the physical problem of an insulated body. Therefore, one cannot expect an accurate prediction of the heat transfer value from the theory. In a more recent paper, Ho and and Probstein[11] have treated the same flow regime with an improved model. The flow equations behind the shock have been obtained by simplifying the Navier-Stokes equations based on the thin shock layer approach. The regular Rankine-Hugoniot shock conditions and the conditions at the wall serve as the boundary conditions of the problem. The heat transfer result from the theory shows the general trend of increase in heat transfer value as the Reynolds number decreases but falls of the order of ten percent based on the boundary layer value below the experimental data.

The inclusion of the effects of the viscous stresses and the heat conduction behind the shock has been studied by Cheng[12]. The flow equations behind the shock have been obtained by simplifying the Navier-Stokes equations consistent with the thin shock layer approximation. Two different schemes have been proposed for the solution of the problem depending on whether the parameter $K^2 = \epsilon\left(\frac{\rho_\infty U_\infty a}{\mu_*}\right)\frac{T_*}{T_o}$ is large or small as described in reference 12. In "Regime I" or the "Vorticity-Interaction" regime as defined by Cheng, the solution has been obtained by integrating the flow equations satisfying the six boundary conditions one of which determines the upper integration limit η_s (boundary layer coordinate). The inviscid theory has been adopted in prescribing the boundary conditions at $\eta = \eta_s$, and the effects of the viscous stresses and the heat conduction behind the shock have not been included here in "Regime I." The theory does not predict the actual detachment distance in a unique manner. The correction term to the inviscid detachment distance presented in reference 12 indicates the displacement effects of the flow field behind the shock, which can only be obtained after performing the integration. Therefore, it is clear that the scheme is reasonably justified only if the displacement effects are small, and we find that this is in agreement with the postulation made in reference 4. In "Regime II" defined by Cheng, the effects of the viscous stresses and the heat conduction behind the shock have been included in the boundary conditions. A perturbation type of approach with parameter characterizing the tangential pressure gradient of the flow has been adopted for the solutions of the problem. Again, the detachment distance does not come into the analysis. Therefore, the fact that the detachment distance and the flow behind the shock are coupled has been ignored. Since essentially the scheme still adopts the concentric shock model, the effect of the shock curvature cannot be observed from the analysis. (Notice that the shock curvature and the detachment distance are different parameters.)

In the present study, a complete matching scheme for the components of the stresses and the heat flux is introduced for the study of the flow field behind the shock. The shock surface or the matching surface can be determined uniquely from the analysis. The detail of the scheme is explained in a later part of this report.

SECTION II

DISCUSSION OF THE PROBLEM

The problem here is to investigate the flow field about a cold blunt nosed body in hypersonic low density stream. We make, as usual, the following justifiable postulations: (1) the disturbed region of the flow field is confined to a distance much smaller than the nose radius of the body; (2) the flow density around the body is much larger than the free stream density, and the continuum formulation is still adopted in the present study. Due to the very large stagnation temperature to wall temperature ratio, the temperature gradient in the direction normal to the wall is much larger than that of the circumferential direction. The temperature jump at the wall cannot be important insomuch as the problem of a cold blunt body in hypersonic flow is considered. Therefore the usual thermal boundary layer remains a good approximation to the temperature distribution, provided appropriate boundary condition can be prescribed at the edge of the temperature layer. The momentum equation of the boundary layer equations is subject to the error that the pressure change across the boundary layer has been ignored. The use of boundary layer equations is justified by the fact that either the normal pressure gradient itself is small, or the boundary layer is thin. Since we are treating the flow field in the shock layer which has a dimension much smaller than the nose radius, it is reasonable to assume that a large portion of the pressure jump is absorbed in the shock transition zone. This is confirmed by the recent work by Cheng[12] where the pressure remains constant along the axis of symmetry has been postulated in the analysis of stagnation region. Therefore, with this discussion in mind, we may seek the solution of the boundary layer equation, with the shock conditions serving appropriately as the boundary conditions of the problem. The systematic analysis of obtaining the shock conditions is discussed in the details of the present work.

SECTION III

SHOCK CONSERVATION EQUATIONS

We assume that the Navier-Stokes equations hold for the range of investigation. The continuity equation, the equations of motion and the energy equation can be expressed in any curvilinear coordinate system suitable for the analysis. For an axially symmetric blunt-nosed body at zero angle of attack, the shock surface close to the axis of symmetry can be approximated by a sphere with the center on the axis. In this axisymmetric spherical polar coordinate system, the system of steady Navier-Stokes equations, neglecting the effects of the body force, can be expressed as follows[16]:

The continuity equation is

$$\frac{\partial}{\partial r}(\rho v) + 2\frac{\rho v}{r} + \frac{1}{r}\frac{\partial}{\partial \theta}(\rho u) + \frac{\rho u}{r}\cot\theta = 0 \qquad \text{(III-1a)}$$

The radial direction of momentum equation is

$$\rho\left[v\frac{\partial v}{\partial r} + \frac{u}{r}\frac{\partial v}{\partial \theta} - \frac{u^2}{r}\right] = \frac{\partial}{\partial r}(\Pi_{rr}) + \frac{1}{r}\frac{\partial}{\partial \theta}(\Pi_{r\theta}) + \frac{1}{r}\left[2\Pi_{rr} - \Pi_{nn} - \Pi_{\theta\theta} + \Pi_{r\theta}\cot\theta\right] \qquad \text{(III-1b)}$$

The circumferential direction of momentum equation is

$$\rho\left[v\frac{\partial u}{\partial r} + \frac{u}{r}\frac{\partial u}{\partial \theta} + \frac{uv}{r}\right] = \frac{\partial}{\partial r}(\Pi_{r\theta}) + \frac{1}{r}\frac{\partial}{\partial \theta}(\Pi_{\theta\theta}) + \frac{1}{r}\left[(\Pi_{\theta\theta} - \Pi_{nn})\cot\theta + 3\Pi_{r\theta}\right] \qquad \text{(III-1c)}$$

The energy equation is

$$\rho\left[v\frac{\partial h}{\partial r} + \frac{u}{r}\frac{\partial h}{\partial \theta}\right] = v\frac{\partial p}{\partial r} + \frac{u}{r}\frac{\partial p}{\partial \theta} + \frac{1}{r}\left[\frac{\partial}{\partial r}\left(kr\frac{\partial T}{\partial r}\right) + \frac{\partial}{\partial \theta}\left(\frac{k}{r}\frac{\partial T}{\partial \theta}\right) + k\left(\frac{\partial T}{\partial r} + \frac{\cot\theta}{r}\frac{\partial T}{\partial \theta}\right)\right] + \Phi \qquad \text{(III-1d)}$$

where

$$\Pi_{rr} = -p + (\mu' - \frac{2}{3}\mu)\left[\frac{1}{r}\frac{\partial u}{\partial \theta} + 2\frac{v}{r} + \frac{u \cot \theta}{r}\right] + (\mu' + \frac{4\mu}{3})\frac{\partial v}{\partial r}$$

$$\Pi_{\theta\theta} = -p + (\mu' - \frac{2}{3}\mu)\left[\frac{\partial v}{\partial r} + \frac{v}{r} + \frac{u \cot \theta}{r}\right] + (\mu' + \frac{4\mu}{3})\left[\frac{1}{r}\frac{\partial u}{\partial \theta} + \frac{v}{r}\right]$$

$$\Pi_{nn} = -p + (\mu' - \frac{2}{3}\mu)\left[\frac{\partial v}{\partial r} + \frac{1}{r}\frac{\partial u}{\partial \theta} + \frac{v}{r}\right] + (\mu' + \frac{4\mu}{3})\left[\frac{v}{r} + \frac{u \cot \theta}{r}\right]$$

$$\Pi_{r\theta} = \mu\left[r\frac{\partial}{\partial r}\left(\frac{u}{r}\right) + \frac{1}{r}\frac{\partial v}{\partial \theta}\right]$$

$$e_{rr} = 2\frac{\partial v}{\partial r}$$

$$e_{\theta\theta} = 2\left[\frac{1}{r}\frac{\partial u}{\partial \theta} + \frac{v}{r}\right]$$

$$e_{nn} = 2\left[\frac{v}{r} + \frac{u \cot \theta}{r}\right]$$

$$e_{r\theta} = r\frac{\partial}{\partial r}\left(\frac{u}{r}\right) + \frac{1}{r}\frac{\partial v}{\partial \theta}$$

$$\Phi = \frac{\mu}{2}\left[e_{rr}^2 + e_{\theta\theta}^2 + e_{nn}^2 + 2e_{r\theta}^2\right] + \frac{1}{2}\left(\frac{\mu'}{2} - \frac{\mu}{3}\right)\left[e_{rr} + e_{\theta\theta} + e_{nn}\right]^2,$$

and v and u are the velocity components along the radial and circumferential directions in the meridian plane; and ρ, p, T, h, μ, μ', k are the density, the pressure, the temperature, the specific enthalpy, the shear and the bulk coefficients of viscosity and the coefficient of heat conduction, respectively.

System of Eqs. (III-1) is approximated by the technique of the order of magnitude analysis developed in reference 14. Introduce for the dependent variables v, u, p, etc. the following expansion scheme in

the shock:

$$v(s, \theta, \nu) = v^{(o)} + \nu v^{(1)} + o(\nu)$$

$$u(s, \theta, \nu) = u^{(o)} + \nu u^{(1)} + o(\nu) \text{ etc.,} \tag{III-2}$$

where s is the stretched radial coordinate across the shock, with the transformations

$$r = R_s + \nu s$$

$$\frac{\partial}{\partial r} = \frac{\partial}{\nu \partial s} \tag{III-3}$$

and R_s is the radius of the shock and $\nu = \frac{\mu_\infty}{\rho_\infty U R_s}$. With these transformations for the independent variables, we can now consider the derivatives of the physical quantities v, u, etc. in the stretched radial direction and the circumferential direction along the shock have the same order of magnitude as explained in reference 13. Substitute Eqs. (III-2) and (III-3) into Eqs. (III-1), equations of successive orders can be obtained consistently with respect to the small parameter ν. In the limit $\nu \to 0$, we obtain the differential equations for the leading order shock solution. Expressed in the nonstretched coordinates they are as follows:

the continuity equation

$$\frac{\partial}{\partial r} (\rho v) = 0 , \tag{III-4a}$$

the radial direction of momentum equation

$$\frac{\partial p}{\partial r} + \rho v \frac{\partial v}{\partial r} = \frac{\partial}{\partial r} \left[(\mu' + \frac{4}{3} \mu) \frac{\partial v}{\partial r} \right] , \tag{III-4b}$$

the circumferential direction of momentum equation

$$\rho v \frac{\partial u}{\partial r} = \frac{\partial}{\partial r}\left[\mu \frac{\partial u}{\partial r}\right], \qquad \text{(III-4c)}$$

and the energy equation

$$\rho v \frac{\partial h}{\partial r} = v \frac{\partial p}{\partial r} + \frac{\partial}{\partial r}\left[k \frac{\partial T}{\partial r}\right] + \left(\mu' + \frac{4}{3}\mu\right)\left[\frac{\partial v}{\partial r}\right]^2 + \mu\left[\frac{\partial u}{\partial r}\right]^2 . \qquad \text{(III-4d)}$$

The terms in Eqs. (III-4) do not involve the derivatives in the circumferential direction, however the dependent variables u, v, p, ρ, T, and h are functions of both the spacial coordinates r and θ.

Referring to Figure 1, Eqs. (III-4) can be integrated along a ray of constant θ from $r = +\infty$ to a point $r = r_1(\theta)$, to be defined later. Eqs. (III-4a), (III-4b), and (III-4c) can be integrated without any difficulty, since both the left-hand and right-hand sides appear in the forms of exact differential. To integrate Eq. (III-4d), we proceed with the following rearrangement, making use of Eqs. (III-4b) and (III-4c):

Multiply Eq. (III-4b) by v

$$v \frac{\partial p}{\partial r} + \rho v\, v \frac{\partial v}{\partial r} = v \frac{\partial}{\partial r}\left[\left(\mu' + \frac{4}{3}\mu\right)\frac{\partial v}{\partial r}\right] = \frac{\partial}{\partial r}\left[\left(\mu' + \frac{4}{3}\mu\right) v \frac{\partial v}{\partial r}\right] - \left(\mu' + \frac{4}{3}\mu\right)\left[\frac{\partial v}{\partial r}\right]^2$$

hence

$$v \frac{\partial p}{\partial r} + \left(\mu' + \frac{4}{3}\mu\right)\left[\frac{\partial v}{\partial r}\right]^2 = \frac{\partial}{\partial r}\left[\left(\mu' + \frac{4}{3}\mu\right) v \frac{\partial v}{\partial r}\right] - \rho v \frac{\partial}{\partial r}\left(\frac{v^2}{2}\right) \qquad \text{(III-5a)}$$

Multiply Eq. (III-4c) by u

$$\rho v\, u \frac{\partial u}{\partial r} = u \frac{\partial}{\partial r}\left[\mu \frac{\partial u}{\partial r}\right] = \frac{\partial}{\partial r}\left[\mu u \frac{\partial u}{\partial r}\right] - \mu\left[\frac{\partial u}{\partial r}\right]^2$$

hence

$$\mu\left[\frac{\partial u}{\partial r}\right]^2 = \frac{\partial}{\partial r}\left[\mu u \frac{\partial u}{\partial r}\right] - \rho v \frac{\partial}{\partial r}\left[\frac{u^2}{2}\right] \qquad \text{(III-5b)}$$

$$\rho v \frac{\partial h}{\partial r} = \frac{\partial}{\partial r}\left[k \frac{\partial T}{\partial r}\right] + \frac{\partial}{\partial r}\left[(\mu' + \frac{4}{3}\mu) v \frac{\partial v}{\partial r}\right] + \frac{\partial}{\partial r}\left[\mu u \frac{\partial u}{\partial r}\right]$$

$$- \rho v \frac{\partial}{\partial r}\left[\frac{v^2}{2}\right] - \rho v \frac{\partial}{\partial r}\left[\frac{u^2}{2}\right]$$

or

$$\rho v \frac{\partial}{\partial r}[h_s] = \frac{\partial}{\partial r}\left\{k \frac{\partial T}{\partial r} + (\mu' + \frac{4}{3}\mu) v \frac{\partial v}{\partial r} + \mu u \frac{\partial u}{\partial r}\right\} \qquad \text{(III-4d')}$$

where h_s is the stagnation enthalpy per unit mass defined as $h_s = h + \frac{u^2+v^2}{2}$. Notice that during this operation no postulation has been made on the transport coefficients k, μ, and μ', they stand, therefore, as from the beginning, as the local gas properties where the local thermodynamic equilibrium is postulated. Integrating Eqs. (III-4a), (III-4b), (III-4c), and (III-4d') we obtain the following:

$$[\rho v]_{r=r_1} = \rho_\infty v_\infty = m \qquad \text{(III-6a)}$$

$$[p + mv - (\mu' + \frac{4}{3}\mu)\frac{\partial v}{\partial r}]_{r=r_1} = p_\infty + m v_\infty \qquad \text{(III-6b)}$$

$$[mu - \mu \frac{\partial u}{\partial r}]_{r=r_1} = m u_\infty \qquad \text{(III-6c)}$$

$$[mh_s - k \frac{\partial T}{\partial r} - (\mu' + \frac{4}{3}\mu) v \frac{\partial v}{\partial r} - \mu u \frac{\partial u}{\partial r}]_{r=r_1} = m h_{s\,\infty} \qquad \text{(III-6d)}$$

where the subscript ∞ in the right-hand side terms denotes that the quantities are evaluated at $r = +\infty$. The left-hand side terms are functions of r_1 and θ, the angle of inclination of the ray. Terms such as v and $\frac{\partial v}{\partial r}$ now can be viewed as independent functions of θ if the integration limit r_1 is prescribed.

Inspecting Eqs. (III-6), we see that they are essentially statements of balances of the mass flux, the components of stresses and the energy flux of the fluid flowing across the shock; and they are the usual leading order shock conditions. Eqs. (III-6) appear essentially the same as Eqs. (5) in reference 14, except where $\frac{\partial u}{\partial r}$ is taken as zero and $u = u_\infty$ const. across the shock, which is the condition necessary in order that u shall be bounded as we integrate along the stretched radial coordinate from $+\infty$ to $-\infty$[14]. Therefore $\frac{\partial u}{\partial r}$ should be retained consistently at $r = r_1$ while $\frac{\partial v}{\partial r}$ and $\frac{\partial T}{\partial r}$ do not vanish. Inspection of Eq. (III-6c) shows that the implication of this is that the effect of change in the tangential component of momentum in a shock does not come in the same order as the effect of the shock structure (the displacement effect).

It has been pointed out in the Introduction that the shock detachment distance and the shock curvature are different parameters. This means that the shock surface near the axis of symmetry, in general, is not concentric with the blunt nosed body where the body shape near the axis can also be approximated by a sphere. For the convenience of study the flow field behind the shock, system of Eqs. (III-6) is transformed and expressed in the body-centered spherical polar coordinate system, where a parameter characterizing the eccentricity of the shock is introduced. This is explained in the next section.

SECTION IV

COORDINATE TRANSFORMATIONS

Referring to Figure 1, we denote the distance between the centers of curvature of the body and of the shock on the axis of symmetry by $O_B O_s = d = eR_B$, where R_B is the radius of the nose on the axis and e is the dimensionless distance. We have then the two spherical polar coordinate systems (r_s, θ_s) and (r_B, θ_B), where the subscripts indicate whether the system is shock-centered or body-centered, respectively.

From the geometry, we have the following transformations:

$$r_s = [d^2 + r_B^2 + 2dr_B \cos\theta_B]^{\frac{1}{2}} \tag{IV-1a}$$

$$\sin\theta_s = r_B \sin\theta_B [d^2 + r_B^2 + 2dr_B \cos\theta_B]^{-\frac{1}{2}} \tag{IV-1b}$$

and

$$r_B = [d^2 + r_s^2 - 2dr_s \cos\theta_s]^{\frac{1}{2}} \tag{IV-2a}$$

$$\sin\theta_B = r_s \sin\theta_s [d^2 + r_s^2 - 2dr_s \cos\theta_s]^{-\frac{1}{2}} \tag{IV-2b}$$

The radial and circumferential components of velocity, the spacial derivatives of the velocity components and the components of the gradient of a scalar quantity at any point P can be transformed from one system to the other by making use of Eqs. (IV-1) and (IV-2). For instance, with the velocity components defined as

$$u_s = r_s \frac{d\theta_s}{dt} \qquad u_B = r_B \frac{d\theta_B}{dt}$$

and

$$v_s = \frac{dr_s}{dt} \qquad v_B = \frac{dr_B}{dt}$$

the circumferential component of velocity referring to the shock system u_s is then

$$u_s = r_s \frac{d}{dt} [\theta_s(r_B, \theta_B)]$$

$$= r_s [\frac{\partial \theta_s}{\partial r_B} \frac{dr_B}{dt} + \frac{\partial \theta_s}{\partial \theta_B} \frac{d\theta_B}{dt}]$$

$$= r_s [v_B \frac{\partial \theta_s}{\partial r_B} + \frac{u_B}{r_B} \frac{\partial \theta_s}{\partial \theta_B}]$$

$$= \frac{v_B[d \sin \theta_B] + u_B[r_B + d \cos \theta_B]}{[d^2 + r_B^2 + 2dr_B \cos \theta_B]^{\frac{1}{2}}}$$

Similarly, the quantities v_s, $\frac{\partial u_s}{\partial r_s}$, $\frac{\partial v_s}{\partial r_s}$, and $\frac{\partial T}{\partial r_s}$ referring to the shock-centered system can be expressed in the new system (r_B, θ_B); they are listed in Appendix A. The parameter $d = O_B O_s$ involved in the transformation can be dtermined uniquely from the analysis, and is explained in the later part of the work.

The system of shock conservation Eqs. (III-6) can now be expressed in the new coordinate system, with terms properly defined as referring to (r_B, θ_B).

The continuity equation is

$$\overline{\rho}\,\overline{v} = -F = -\frac{e + (1+y)\cos \theta}{[e^2 + (1+y)^2 + 2e(1+y)\cos \theta]^{\frac{1}{2}}} \qquad \text{(IV-3a)}$$

The radial component of momentum equation is

$$\left\{\frac{\Gamma-1}{\Gamma}\,\bar{\rho}\left[\bar{h}_s-\frac{1}{2}\left(\bar{v}^2+\bar{u}^2\right)\right]-\bar{p}_\infty\right\}\left\{e^2+(1+y)^2+2e(1+y)\cos\theta\right\}$$

$$=\left[e+(1+y)\cos\theta\right]^2+\left[e+(1+y)\cos\theta\right]\left\{(1+y+e\cos\theta)\,\bar{v}-(e\sin\theta)\,\bar{u}\right\}$$

$$+\epsilon_2\left\{\left(\frac{e\sin\theta}{1+y}\right)\left[(e\sin\theta)\,\bar{v}+(1+y-e\cos\theta)\,\bar{u}\right]+\frac{\partial\bar{v}}{\partial y}\left[1+y+e\cos\theta\right]^2\right.$$

$$\left.-\frac{\partial\bar{u}}{\partial y}(e\sin\theta)[1+y+e\cos\theta]+\left(\frac{1}{1+y}\right)\frac{\partial\bar{u}}{\partial\theta}[e^2\sin^2\theta]-\left(\frac{e\sin\theta}{1+y}\right)\frac{\partial\bar{v}}{\partial\theta}[1+y+e\cos\theta]\right\} \qquad \text{(IV-3b)}$$

The circumferential component of momentum equation is

$$\left[e+(1+y)\cos\theta\right]\left\{[e\sin\theta]\bar{v}+[1+y+e\cos\theta]\,\bar{u}\right\}$$

$$+\epsilon_1\left\{\left(\frac{e\sin\theta}{1+y}\right)\left[(e\sin\theta)\,\bar{u}-(1+y+e\cos\theta)\,\bar{v}\right]\right.$$

$$-\left(\frac{e^2\sin^2\theta}{1+y}\right)\frac{\partial\bar{v}}{\partial\theta}-\left(\frac{e\sin\theta}{1+y}\right)[1+y+e\cos\theta]\,\frac{\partial\bar{u}}{\partial\theta}$$

$$\left.+(e\sin\theta)\,[1+y+e\cos\theta]\,\frac{\partial\bar{v}}{\partial y}+[1+y+e\cos\theta]^2\,\frac{\partial\bar{u}}{\partial y}\right\}$$

$$=(1+y)\sin\theta\,[e+(1+y)\cos\theta] \qquad \text{(IV-3c)}$$

The energy equation is

$$\left[e+(1+y)\cos\theta\right]\left\{e^2+(1+y)^2+2e(1+y)\cos\theta\right\}\left\{\bar{h}_s-\bar{h}_{s\,\infty}\right\}$$

$$+\left(\frac{\epsilon_1}{P_{r_1}}\right)\left[e^2+(1+y)^2+2e(1+y)\cos\theta\right]\left\{(1+y+e\cos\theta)\,\frac{\partial\bar{h}_s}{\partial y}-\left(\frac{e\sin\theta}{1+y}\right)\frac{\partial\bar{h}_s}{\partial\theta}\right\}$$

$$+ \left(\frac{\epsilon_2}{P_{r_2}}\right) \left\{P_{r_2} - 1\right\} \left\{(1+y+e\cos\theta)\,\bar{v} - (e\sin\theta)\,\bar{u}\right\} \cdot$$

$$\left\{\left(\frac{e\sin\theta}{1+y}\right)\left[(e\sin\theta)\,\bar{v} + (1+y-e\cos\theta)\,\bar{u}\right] + \frac{\partial\bar{v}}{\partial y}\left[1+y+e\cos\theta\right]^2\right.$$

$$- \frac{\partial\bar{u}}{\partial y}(e\sin\theta)\left[1+y+e\cos\theta\right] + \left(\frac{e^2\sin^2\theta}{1+y}\right)\frac{\partial\bar{u}}{\partial\theta} - \left(\frac{e\sin\theta}{1+y}\right)\frac{\partial\bar{v}}{\partial\theta}\left[1+y+e\cos\theta\right]\Big\}$$

$$+ \left(\frac{\epsilon_1}{P_{r_1}}\right) \left\{P_{r_1} - 1\right\} \left\{(e\sin\theta)\,\bar{v} + (1+y+e\cos\theta)\,\bar{u}\right\} \cdot$$

$$\left\{\left(\frac{e\sin\theta}{1+y}\right)\left[(e\sin\theta)\,\bar{u} - (1+y+e\cos\theta)\,\bar{v}\right] - \left(\frac{e^2\sin^2\theta}{1+y}\right)\frac{\partial\bar{v}}{\partial\theta}\right.$$

$$- \left(\frac{e\sin\theta}{1+y}\right)\frac{\partial\bar{u}}{\partial\theta}\left[1+y+e\cos\theta\right] + (e\sin\theta)\left[1+y+e\cos\theta\right]\frac{\partial\bar{v}}{\partial y}$$

$$\left.+ \left[1+y+e\cos\theta\right]^2\frac{\partial\bar{u}}{\partial y}\right\} = 0 \qquad \text{(IV-3d)}$$

All the bar quantities in Eqs. (IV-3) refer to those nondimensionalized with respect to the free stream quantities; they are defined as

$$\bar{u} = \frac{u}{U}\ ;\ \bar{v} = \frac{v}{U}\ ;\ \bar{\rho} = \frac{\rho}{\rho_\infty}\ ;\ \bar{h}_s = \frac{h_s}{U^2}\ ;\ \bar{h}_{s\,\infty} = \frac{h_{s\,\infty}}{U^2}\ ;\ \bar{p}_\infty = \frac{p_\infty}{\rho_\infty U^2}$$

and

$$y = \frac{r-R_B}{R_B}\ ;\quad e = \frac{d}{R_B}$$

$$\Gamma = \frac{c_p}{c_v}\ ;\ P_{r_1} = \frac{\mu_1 c_p}{k}\ ;\ P_{r_2} = \frac{\mu_2 c_p}{k}\ ;\ \epsilon_1 = \frac{\mu_1}{\rho_\infty U R_B}\ ;\ \epsilon_2 = \frac{\mu_2}{\rho_\infty U R_B}$$

and

$$\mu_1 = \mu \; ; \; \mu_2 = \mu' + \frac{4}{3}\mu \, .$$

Again Eqs. (IV-3) are evaluated at $y = y_1(\theta)$, where the only independent variable is θ.

SECTION V

METHOD OF SOLUTION

Using the boundary layer approximation near the wall, the basic equations of single species laminar boundary layer flow can be expressed as follows:

Continuity Equation

$$\frac{\partial}{\partial y}(\bar{\rho}\,\bar{v}) + \frac{\partial}{\partial \theta}(\bar{\rho}\,\bar{u}) + \bar{\rho}\,\bar{u}\cot\theta = 0 \qquad \text{(V-1a)}$$

Momentum Equation

$$\bar{\rho}\left(\bar{u}\frac{\partial u}{\partial \theta} + \bar{v}\frac{\partial u}{\partial y}\right) = -\frac{d\bar{p}_e}{d\theta} + \epsilon\frac{\partial}{\partial y}\left(\bar{\mu}\frac{\partial \bar{u}}{\partial y}\right) \qquad \text{(V-1b)}$$

Energy Equation

$$\bar{\rho}\left(\bar{u}\frac{\partial \bar{h}_s}{\partial \theta} + \bar{v}\frac{\partial \bar{h}_s}{\partial y}\right) = \epsilon\left\{\frac{\partial}{\partial y}\left(\frac{\bar{\mu}}{P_r}\frac{\partial \bar{h}_s}{\partial y}\right) + \frac{\partial}{\partial y}\left[\bar{\mu}\left(1-\frac{1}{P_r}\right)\frac{\partial}{\partial y}\left(\frac{\bar{u}^2}{2}\right)\right]\right\} \qquad \text{(V-1c)}$$

Eqs. (V-1) are the same as those appearing in reference 1 without considering the diffusion phenomena, except here all the dependent and the independent variables are normalized in consistence with Eqs. (IV-3). The body shape is approximated by a sphere with radius R_B, and $y = \frac{r-R_B}{R_B}$. The problem remains now to seek the solution of Eqs. (V-1) satisfying the usual three boundary conditions, the temperature distribution, and the non-slip boundary conditions at the wall, and the four shock conservation Eqs. (IV-3) at a point yet to be determined. Notice that four outer boundary conditions appear here as compared with the usual three, - the inviscid velocity and density distribution at the wall and the stagnation enthalpy[1] prescribed at the edge of a thin boundary layer. This extra condition suffices to determine the upper integration limit $y = y_1$, or more specifically, the detachment distance of the shock. The solution of Eqs. (V-1), in general, can be obtained by machine

integration with suitable transformation for the dependent and the independent variables. However, the problem can be solved more easily by using a technique similar to that employed in reference 4. In this technique, the physical quantities $\bar{u}$, $\bar{v}$, $\bar{\rho}$, $\bar{h}_s$ and their radial derivatives can be expressed in terms of the similarity solutions and the fictitious outer flow quantities $\bar{u}_e$, $\bar{\rho}_e$, and $\bar{h}_{se}$, which in turn can be determined uniquely from the present analysis (Figure 2).

We start with the Lees' transformation[1]

$$\eta = \frac{\rho_e u_e}{\sqrt{2\xi}} \int_0^y R_B^2 \sin\theta \left(\frac{\rho}{\rho_e}\right) dy \qquad \text{(V-2a)}$$

$$\xi = \int_0^\theta \rho_e u_e \mu_e R_B^3 \sin^2\theta d\theta \qquad \text{(V-2b)}$$

and

$$\rho u R_B^2 \sin\theta = \frac{\partial \psi}{\partial y} \qquad \text{(V-2c)}$$

$$\rho v R_B^2 \sin\theta = -\frac{\partial \psi}{\partial \theta} \qquad \text{(V-2d)}$$

$$\psi(\theta, y) = \sqrt{2\xi}\, f(\eta) \qquad \text{(V-2e)}$$

$$h_s/h_{se} = g(\eta) \quad , \qquad \text{(V-2f)}$$

where quantities with subscript e refer to the outer flow quantities of the boundary layer (i.e., at $\eta = \infty$) with the boundary conditions as given in reference 1, and y is the dimensionless radial coordinate. Consistent with Eqs. (V-2), any physical quantity among $\bar{u}$, $\bar{v}$, $\bar{\rho}$ and $\bar{h}_s$ and their spacial derivatives at $y = y_1$ (or $\eta = \eta_1$) can be expressed in terms of the similarity solutions f and g and ρ_e, u_e, h_{se}. For instance

$$\bar{u}_1 = [\bar{u}]_{y=y_1} = \bar{u}_e \left.\frac{df}{d\eta}\right|_{\eta=\eta_1} = \bar{u}_e f_1'$$

$$\left[\frac{\partial \bar{u}}{\partial y}\right]_1 = \left[\frac{\partial \bar{u}}{\partial y}\right]_{y=y_1} = \frac{\bar{u}_e^2 \bar{\rho}_e \sin\theta f_1''}{\sqrt{2\epsilon \bar{\xi}\, g_1}}$$

$$\left[\frac{\partial \bar{u}}{\partial \theta}\right]_1 = f_1' \left[\frac{\partial \bar{u}_e}{\partial \theta}\right] + \bar{u}_e f_1'' \eta_1 \left[\frac{\frac{\partial}{\partial \theta}(\sin\theta \bar{\rho}_e \bar{u}_e)}{\sin\theta\, \bar{\rho}\, \bar{u}} - \frac{\bar{\rho}_e \bar{u}_e \bar{\mu}_e \sin^2\theta}{2\bar{\xi}}\right]$$

$$\bar{\xi} = \int_0^\theta \bar{\rho}_e \bar{u}_e \bar{\mu}_e \sin^2\theta d\theta \quad ,$$

where the bar quantities refer to the quantities nondimensionalized with respect to the free stream values; and f_1' and f_1'' denote, respectively, first and second derivatives of f with respect to η at $\eta = \eta_1$. Therefore, the shock conservation Eqs. (IV-3) can readily be transformed according to Eqs. (V-2). And, together with Eq. (V-2a), this forms a complete set of five equations for the new variables $\bar{u}_e(\theta)$, $\bar{\rho}_e(\theta)$, $\bar{h}_{se}(\theta)$, $y_1(\theta)$, and $\eta_1(\theta)$.

For the five equations to hold near the axis of symmetry, the following expansion schemes around $\theta=0$ for all the variables can be introduced for further simplification of the problem:

$$\bar{u}_e(\theta) = {}_1\bar{u}_e\, \theta + {}_3\bar{u}_e\, \theta^3 \qquad \text{(V-3a)}$$

$$\bar{\rho}_e(\theta) = {}_0\bar{\rho}_e + {}_2\bar{\rho}_e\, \theta^2 \qquad \text{(V-3b)}$$

$$\bar{h}_{se}(\theta) = {}_0\bar{h}_{se} + {}_2\bar{h}_{se}\, \theta^2 \qquad \text{(V-3c)}$$

$$\eta_1(\theta) = {}_0\eta_1 + {}_2\eta_1\, \theta^2 \qquad \text{(V-3d)}$$

$$y_1(\theta) = {}_0y_1 + {}_2y_1\, \theta^2 \qquad \text{(V-3e)}$$

Introducing Eqs. (V-3) into the transformed shock conservation equations,

and collecting terms of equal powers of θ^0 and θ^2, we obtain finally the ten algebraic equations for the ten unknown coefficients: ${}_1\bar{u}_e$, ${}_3\bar{u}_e$, ${}_0\bar{\rho}_e$, ${}_2\bar{\rho}_e$, ${}_0\bar{h}_{se}$, ${}_2\bar{h}_{se}$, ${}_0\eta_1$, ${}_2\eta_1$, ${}_0y_1$, and ${}_2y_1$ (or e). They are the equations on the axis (coefficients of θ^0 terms)

$$[2\epsilon\bar{\mu}_e\ {}_0\bar{\rho}_e\ {}_1\bar{u}_e]^{\frac{1}{2}}\ f_1 = 1 \tag{V-4a}$$

$${}_0y_1 = \frac{\int_0^{{}_0\eta_1} g\,d\eta}{2f_1\ {}_0\bar{\rho}_e\ {}_1\bar{u}_e} \tag{V-4b}$$

$$(1+{}_0y_1)\left\{[{}_1\bar{u}_e\ {}_0\bar{\rho}_e]f_1' + \epsilon_1[{}_1\bar{u}_e\ {}_0\bar{\rho}_e]^2\ 2f_1f_1''\right\} + e\left\{[({}_1\bar{u}_e\ {}_0\bar{\rho}_e)f_1' - g]\right. \tag{V-4c}$$

$$\left. -\epsilon_1\left[\frac{({}_1\bar{u}_e\ {}_0\bar{\rho}_e)f_1' - g_1}{1+{}_0y_1} + ({}_1\bar{u}_e\ {}_0\bar{\rho}_e)(2f_1')\left(1+\frac{f_1g_1'}{f_1'g_1}\right) - ({}_1\bar{u}_e\ {}_0\bar{\rho}_e)^2(2f_1f_1'')\right]\right\} = (1+{}_0y_1)\,{}_0\bar{\rho}_e$$

$$1 + \bar{p}_\infty = \frac{\Gamma-1}{\Gamma}\ {}_0\bar{\rho}_e\ {}_0\bar{h}_{se} + \frac{\Gamma+1}{2\Gamma}\left[\frac{g_1}{{}_0\rho_e}\right] + \epsilon_2\ {}_1\bar{u}_e\left[2f_1' + 2f_1\ \frac{g_1'}{g_1}\right] \tag{V-4d}$$

$$[\bar{h}_{s\,\infty} - {}_0\bar{h}_{se}\ g_1] = \epsilon_2\ {}_0\bar{h}_{se}\ {}_0\bar{\rho}_e\ {}_1\bar{u}_e\left[\frac{2f_1g_1'}{g_1}\right]\ , \tag{V-4e}$$

and the equations away from the axis (coefficients of θ^2 terms)

$$\begin{Vmatrix} K_1 & K_2 & K_3 & K_4 & K_5 \\ Y_1 & Y_2 & Y_3 & Y_4 & Y_5 \\ \Theta_1 & \Theta_2 & \Theta_3 & \Theta_4 & \Theta_5 \\ P_1 & P_2 & P_3 & P_4 & P_5 \\ E_1 & E_2 & E_3 & E_4 & E_5 \end{Vmatrix} \begin{Vmatrix} {}_3\bar{u}_e \,/\, {}_1\bar{u}_e \\ {}_2\bar{\rho}_e \,/\, {}_0\bar{\rho}_e \\ {}_2\bar{h}_{se} \,/\, {}_0\bar{h}_{se} \\ {}_2\eta_1 \\ 1 \end{Vmatrix} = 0 \qquad \text{(V-5a-e)}$$

The coefficients K_i, Y_i, Θ_i, P_i, E_i $(i = 1, 2, 3, 4, 5)$ of the linear Eqs. (V-5) are functions of ${}_1\bar{u}_e$, ${}_0\bar{\rho}_e$, ${}_0\bar{h}_{se}$, ${}_0\eta_1$, ${}_0y_1$ and ${}_2y_1$ (or e); they are listed in Appendix B. All the notations appearing here are defined in consistence with Eqs. (V-3), (V-2), and (IV-3). Notice that in Eqs. (V-4) and (V-5), the quantity $e = \frac{O_B O_s}{R_B}$ does not appear as an extra variable other than ${}_2y_1$. Since, from the matching surface

$$\bar{r}_1(\theta) = \frac{r_1(\theta)}{R_B} = 1 + y_1(\theta) = (1 + {}_0y_1) + {}_2y_1\ \theta^2$$

and

$$(1 + {}_0y_1 + e) \cong (\text{shock radius at } \theta = 0) \cong \left. \frac{[\bar{r}_1^2 + (\frac{d\bar{r}_1}{d\theta})^2]^{\frac{3}{2}}}{\bar{r}_1^2 + 2(\frac{d\bar{r}_1}{d\theta})^2 - \bar{r}_1 \frac{d^2\bar{r}_1}{d\theta^2}} \right|_{\theta=0},$$

it can easily be derived that

$${}_2y_1 = \frac{e}{2}\left[\frac{1 + {}_0y_1}{1 + {}_0y_1 + e}\right]$$

Inspection of Eqs. (V-4) and (V-5) shows that the two sets of equations are coupled in a sense that Eqs. (V-4) involve the six variables ${}_1\bar{u}_e$, ${}_0\bar{\rho}_e$, ${}_0\bar{h}_{se}$, ${}_0\eta_1$, ${}_0y_1$ and e while Eqs. (V-5) involve all the ten variables in which $\frac{{}_3\bar{u}_e}{{}_1\bar{u}_e}$, $\frac{{}_2\bar{\rho}_e}{{}_0\bar{\rho}_e}$, $\frac{{}_2\bar{h}_{se}}{{}_0\bar{h}_{se}}$, and ${}_2\eta_1$ appear linearly. This suggests the following iteration procedure for the solution of the problem: for prescribed initial value of e, values of ${}_1\bar{u}_e$, ${}_0\bar{\rho}_e$, ${}_0\bar{h}_{se}$, ${}_0\eta_1$, and ${}_0y_1$ can be determined by solving Eqs. (V-4); then the new value of e can be obtained by solving one of the five equations in Eqs. (V-5) for the next cycle of iteration. The numerical example is presented in the next section.

Inspection of Eqs. (V-4) and (V-5) shows that the two sets of equations are coupled in a sense that Eqs. (V-4) involve the six variables ${}_1\bar{u}_e$, ${}_0\bar{\rho}_e$, ${}_0\bar{h}_{se}$, ${}_0\eta_1$, ${}_0y_1$ and e while Eqs. (V-5) involve all the ten variables in which $\frac{{}_3\bar{u}_e}{{}_1\bar{u}_e}$, $\frac{{}_2\bar{\rho}_e}{{}_0\bar{\rho}_e}$, $\frac{{}_2\bar{h}_{se}}{{}_0\bar{h}_{se}}$, and ${}_2\eta_1$ appear linearly. This suggests the following iteration procedure for the solution of the problem: for prescribed initial value of e, values of ${}_1\bar{u}_e$, ${}_0\bar{\rho}_e$, ${}_0\bar{h}_{se}$, ${}_0\eta_1$, and ${}_0y_1$ can be determined by solving Eqs. (V-4); then the new value of e can be obtained by solving one of the five equations in Eqs. (V-5) for the next cycle of iteration. The numerical example is presented in the next section.

SECTION VI

NUMERICAL EXAMPLE AND DISCUSSION OF RESULTS

Eqs. (V-4) and (V-5) are applied in the specific calculation for the case of $M_\infty = 5.7$ and T_o = free stream stagnation temperature = 2100°R. In performing the computation, the cold wall approximation has been used for the enthalpy profile $g = f'$, and numerical values for the Blasius velocity profile f have been obtained from reference 17. The linear temperature-coefficient of viscosity law has been assumed. (Notice that the use of Blasius velocity profile does not imply the present scheme is restricted only to zero tangential pressure gradient. In fact the present analysis is completely general for various tangential pressure gradient imbedded in the momentum equation of the boundary layer equations.)

The results are presented in Tables I and II for the range of Reynolds number $Re_s = \frac{\rho_s' \sqrt{h_{s\infty}}\, R_B}{\mu_t}$ (reference 4) from 20 to 400. Where the $\overline{{}_o\rho_1}$ and the $\overline{h}_{s1}$ are, respectively, the density and the stagnation enthalpy at the matching point on the axis. They are plotted as functions of the Reynolds number in Figure 3. It is interesting to observe that the value of $\overline{{}_o\rho_1}$ decreases as Re_s increases and that it approaches the value corresponding to that across a discontinuous shock ($\overline{{}_o\rho_1} = 6.22626$ based on $M_\infty = 5.7$ and $\Gamma = 1.325$ after the shock). The value of $\overline{{}_o\rho_1}$ increases rapidly as the Reynolds number decreases; the unbounded trend is due to the fact that the cold wall approximation has been used in the calculation and $\overline{{}_o\rho_1} = \overline{{}_o\rho_e}/g_1 = \overline{{}_o\rho_e}/f'$. The stagnation enthalpy at the matching point $\overline{{}_oh_{s1}}$ increases as the Reynolds number increases, and approaches the value of the free stream stagnation enthalpy. This indicates the fact that the heat flux in the radial direction after the shock becomes more and more important as the Reynolds number decreases. The results of $\overline{{}_2\rho_e}/\overline{{}_o\rho_e}$ and $\overline{{}_2h_{se}}/\overline{{}_oh_{se}}$ are also shown in Table I. The negative value indicates both the stagnation enthalpy and density decay along the circumferential direction. The rapidness of the decay can also be observed from the magnitude of the coefficients. As both

$_2\bar{\rho}_e/_0\bar{\rho}_e$ and $_2\bar{h}_{se}/_0\bar{h}_{se}$ approach zero as the Reynolds number increases, one can easily observe that the concept of the constant inviscid density distribution is reasonably justified at high Mach number and high Reynolds number. The shock eccentricity e is plotted against $_0\eta_1$ as shown in Figure 4. The matching distance $_0y_1$ on the axis is plotted agains Re_s as shown in Figure 5. The value of $_0y_1$ stays within 3 percent for the range of Re_s from 50 to 400, and is of the order of one-half of the inviscid detachment distance. This can probably be explained as the shock is merging into the boundary layer. The accuracy of this result has yet to be verified with the experimental data at this Mach number. The rapid decrease of $_0y_1$ at $Re_s = 20$ indicates the probable range of application of the present scheme, as it seems to be unrealistic to extend the range of continuum approach any further.

In terms of the boundary layer language, the surface heat transfer value is[1]

$$\dot{q}_w = -k_w \frac{\partial T}{\partial y}\Big)_w = -\frac{k_w}{c_{p_w}} \frac{\partial h}{\partial y}\Big)_w = -\frac{k_w}{c_{p_w}} \frac{\partial h_s}{\partial y}\Big)_w$$

$$= -\frac{k_w}{c_{p_w}} h_{se} g'(o) \left(\frac{\partial \eta}{\partial y}\right)_w = -\frac{k_w}{c_{p_w}} \frac{\rho_w u_e r_o}{(2\tilde{s})^{\frac{1}{2}}} h_{se} g'(o)$$

For the same wall temperature, the heat transfer ratio based on the boundary layer value at the stagnation point can easily be derived. It is

$$\frac{\dot{q}}{\dot{q}_{B.L.}} = \left(\frac{{}_0\bar{\rho}_e}{{}_0\bar{\rho}'_s}\right) \left(\frac{{}_1\bar{u}_e}{{}_1\bar{u}_o}\right)^{\frac{1}{2}} \left(\frac{{}_0\bar{h}_{se}}{\bar{h}_{s\infty}}\right)$$

where $_0\bar{\rho}'_s$ is the normalized inviscid stagnation density after the discontinuous shock, and $_1\bar{u}_o$ is the inviscid velocity distribution based on reference 1. For $M_\infty = 5.7$ and $\Gamma = 1.325$, we have

$$\overline{{}_{o}\rho_{s}'} = 6.67518 \qquad \overline{u}_{1o} = 0.52123 .$$

The result of $\frac{\dot{q}}{\dot{q}_{B.L.}}$ is shown in Table II. Figure 4.1 of reference 15 is reproduced in Figure 6 for comparison of the present theory with the theory developed in reference 12, as well as with the experimental data of references 4, 18, and 19. The plot shows a slight improvement on the heat transfer than the theory developed in reference 12 in the range of application of the present scheme. This indicates that the shock eccentricity does not play a very important role as far as heat transfer value is concerned. The theory breaks down beyond the point where Re_s is of the order of 400, as apparently one cannot expect the "direct matching" to be a realistic scheme.

The heat transfer value is also converted and expressed in $C_H\sqrt{Re_s}$, where the dimensionless heat transfer value $C_H = \frac{q}{\rho_\infty U(H_{s\infty} - H_w)}$. The result is plotted against Re_s as shown in Figure 7. Some of the experimental results of references 4, 18, 19, and 20 are also included for comparison. It is seen that at the large Reynolds number end, the difference on the heat transfer value between the theories of references 4 and 14 is only of the order of two percent when the absolute scale is used.

SECTION VII

CONCLUSION

It was found that the heat fluxes and stress components behind the shock have strong influences on the flow field around the body in the range of Reynolds number of the present study. The heat transfer value decreases monotonically towards the free molecular value as the Reynolds number decreases. The shock eccentricity was found to have very little influence on the heat transfer value. The flow density at the matching surface increases rapidly as the Reynolds number decreases. On the other hand, the stagnation enthalpy at the matching surface decreases as the Reynolds number decreases. Both the stagnation enthalpy and the density at the matching surface yield the regular Rankine-Hugoniot values at the large Reynolds number end.

SECTION VIII

REFERENCES

1. Lees, L.: Laminar Heat Transfer Over Blunt-Nosed Bodies at Hypersonic Flight Speeds. Jet Propulsion, 26, 4, pp. 259-269, 274, April 1956.

2. Fay, J. A. and Riddell, F. R.: Theory of Stagnation Point Heat Transfer in Dissociated Air. J. Aero. Sci., 25, 2, February 1958.

3. Ferri, A. and Libby, P. A.: Note on an Interaction Between the Boundary Layer and the Inviscid Flow. J. Aero. Sci., 21, 2, p. 130, February 1954.

4. Ferri, A., Zakkay, V., and Ting, L.: Blunt-Body Heat Transfer at Hypersonic Speed and Low Reynolds Numbers. J. Aero. Sci., 28, 12, pp. 962-971, December 1961.

5. Ferri, A. and Zakkay, V.: Measurements of Stagnation Point Heat Transfer at Low Reynolds Numbers. J. Aero. Sci., 29, 7, pp. 847-850, July 1962.

6. Sedov, L. I., Michailova, M. P., and Chernyi, G. G.: On the Influences of Viscosity and Heat Conduction on the Gas Flow Behind a Strong Shock Wave. Vestnik Moskovskovo Universiteta, pp. 95-100, No. 3, 1953. (English translation WADC TN 59-349, by Ronald F. Probstein.)

7. Van Dyke, M.: Second Order Compressible Boundary-Layer Theory with Application to Blunt Bodies in Hypersonic Flow. SUDAER No. 112, Department of Aeronautical Engineering, Stanford University, July 1961.

8. Hayes, W. D. and Probstein, R.: Hypersonic Flow Theory. Academic Press, New York, 1959.

9. Probstein, R. F.: Shock Wave and Flow Field Development in Hypersonic Re-entry. ARS J., 31, 2, pp. 185-194, February 1961.

10. Probstein, R. F. and Kemp, N. H.: Viscous Aerodynamic Characteristics in Hypersonic Rarefied Gas Flow. J. Aero. Sci., 27, 3, March 1960.

11. Ho, H. T. and Probstein, R. F.: The Compressible Viscous Layer in Rarefied Hypersonic Flow. Brown University, ARL TN 60-130, August 1960.

12. Cheng, H. K.: Hypersonic Shock-Layer Theory of the Stagnation Region at Low Reynolds Number. Proc. Heat Transfer and Fluid Mechanics Institute, University of Southern California, Stanford University Press, Stanford, California, p. 161, June 1961.

13. Ludford, G. S. S.: The Boundary Layer Nature of Shock Transition in a Real Fluid. Quart. Appl. Math., X, 1, April 1952.

14. Chow, R. R. and Ting, L.: Higher Order Theory of Curved Shock. J. Aero. Sci., 28, 5, pp. 428-430, May 1961.

15. Cheng, H. K.: The Blunt-Body Problem in Hypersonic Flow at Low Reynolds Number. Presented at the IAS 31st Annual Meeting, New York, IAS Paper No. 63-92, January 1963.

16. Tsien, H. S.: The Equations of Gas Dynamics. High Speed Aerodynamics and Jet Propulsion, Vol. III - Fundamentals of Gas Dynamics, H. W. Emmons, Ed., Princeton Univ. Press, Princeton, New Jersey, 1958.

17. Libby, P. A. and Fox, H.: Some Perturbation Solutions in Laminar Boundary Layer Theory, Part I - The Momentum Equation. Polytechnic Institute of Brooklyn, PIBAL Report No. 752, August 1962.

18. Ferri, A. and Zakkay, V.: Measurement of Stagnation Point Heat Transfer at Low Reynolds Numbers. J. Aero. Sci., 29, 7, p. 847, July 1962.

19. Wittliff, C. E. and Wilson, M. R.: Low Density Stagnation Point Heat Transfer in the Hypersonic Shock Tunnels. ARS J., 32, 2, pp. 275-276, February 1962.

20. Wittliff, C. E. and Wilson, M. R.: Low-Density Stagnation-Point Heat Transfer in Hypersonic Air Flow. Cornell Aeronautical Lab., Inc., Rep. AF-1270-A-3, ARL TR 60-333, December 1960.

APPENDIX A

TRANSFORMATIONS BETWEEN SHOCK-CENTERED SPHERICAL COORDINATE SYSTEM AND BODY-CENTERED SPHERICAL COORDINATE SYSTEM

1. TRANSFORMATIONS OF THE SPACIAL COORDINATES

From the geometry (referring to Figure 1), the coordinate transformations between the two systems (r_s, θ_s) and (r_B, θ_B) are

$$r_s = [d^2 + r_B^2 + 2dr_B \cos \theta_B]^{\frac{1}{2}} \tag{II-1a}$$

$$\sin \theta_s = r_B \sin \theta_B [d^2 + r_B^2 + 2dr_B \cos \theta_B]^{-\frac{1}{2}} \tag{II-1b}$$

and

$$r_B = [d^2 + r_s^2 - 2dr_s \cos \theta_s]^{\frac{1}{2}} \tag{II-2a}$$

$$\sin \theta_B = r_s \sin \theta_s [d^2 + r_s^2 - 2dr_s \cos \theta_s]^{-\frac{1}{2}} \tag{II-2b}$$

where d is the distance between the centers O_B and O_s, and the subscripts B and s refer to the coordinate system and are body-centered or shock-centered, respectively.

2. TRANSFORMATIONS OF THE VELOCITY COMPONENTS

The radial and circumferential velocity components are defined as

$$u_s = r_s \frac{d\theta_s}{dt} \qquad u_B = r_B \frac{d\theta_B}{dt}$$

and

$$v_s = \frac{dr_s}{dt} \qquad v_B = \frac{dr_B}{dt}$$

Then,

$$u_s = r_s \frac{d}{dt} [\theta_s(r_B, \theta_B)]$$

$$= r_s \left[\frac{\partial \theta_s}{\partial r_B} \frac{dr_B}{dt} + \frac{\partial \theta_s}{\partial \theta_B} \frac{d\theta_B}{dt}\right]$$

$$= r_s \left[v_B \frac{\partial \theta_s}{\partial r_B} + \frac{u_B}{r_B} \frac{\partial \theta_s}{\partial \theta_B}\right]$$

$$u_s = \frac{v_B[d \sin \theta_B] + u_B[r_B + d \cos \theta_B]}{[d^2 + r_B^2 + 2dr_B \cos \theta_B]^{\frac{1}{2}}} \qquad \text{(A-1)}$$

Similarly, we obtain

$$v_s = \frac{v_B[r_B + d \cos \theta_B] - u_B[d \sin \theta_B]}{[d^2 + r_B^2 + 2dr_B \cos \theta_B]^{\frac{1}{2}}} \qquad \text{(A-2)}$$

3. TRANSFORMATIONS OF THE DERIVATIVES OF THE VELOCITY COMPONENTS

$$\frac{\partial u_s}{\partial r_s} = \left(\frac{\partial \theta_B}{\partial r_s}\right) \frac{\partial u_s}{\partial \theta_B} + \left(\frac{\partial r_B}{\partial r_s}\right) \frac{\partial u_s}{\partial r_B}$$

$$\frac{\partial \theta_B}{\partial r_s} = \frac{-d \sin \theta_s}{[r_s^2 + d^2 - 2dr_s \cos \theta_s]} = \frac{-d \sin \theta_B}{r_B [r_B^2 + d^2 + 2dr_B \cos \theta_B]^{\frac{1}{2}}}$$

and

$$\frac{\partial r_B}{\partial r_s} = \frac{r_B + d \cos \theta_B}{[r_B^2 + d^2 + 2dr_B \cos \theta_B]^{\frac{1}{2}}}$$

Making use of Eq. (A-1), we obtain

$$\begin{aligned}\frac{\partial u_s}{\partial r_s} = {} & \frac{d \sin \theta_B}{r_B (r_B^2 + d^2 + 2dr_B \cos \theta_B)} [(d \sin \theta_B) u_B - (r_B + d \cos \theta_B) v_B] \\ & + [r_B^2 + d^2 + 2dr_B \cos \theta_B]^{-1} \left\{ [r_B + d \cos \theta_B]^2 \frac{\partial u_B}{\partial r_B} \right. \\ & + (d \sin \theta_B) [r_B + d \cos \theta_B] \frac{\partial v_B}{\partial r_B} \\ & \left. - \left(\frac{d \sin \theta_B}{r_B}\right) [r_B + d \cos \theta_B] \frac{\partial u_B}{\partial \theta_B} - \left(\frac{d^2 \sin^2 \theta_B}{r_B}\right) \frac{\partial v_B}{\partial \theta_B} \right\}\end{aligned} \tag{A-3}$$

Similarly, we obtain

$$\begin{aligned}\frac{\partial v_s}{\partial r_s} = {} & \frac{d \sin \theta_B}{r_B (r_B^2 + d^2 + 2dr_B \cos \theta_B)} [(d \sin \theta_B) v_B + (r_B - d \cos \theta_B) u_B] \\ & + [r_B^2 + d^2 + 2dr_B \cos \theta_B]^{-1} \left\{ [r_B + d \cos \theta_B]^2 \frac{\partial v_B}{\partial r_B} \right.\end{aligned}$$

$$- (d \sin \theta_B) [r_B + d \cos \theta_B] \frac{\partial u_B}{\partial r_B}$$

$$+ \left(\frac{d^2 \sin^2 \theta_B}{r_B}\right) \frac{\partial u_B}{\partial \theta_B} - \left(\frac{d \sin \theta_B}{r_B}\right) [r_B + d \cos \theta_B] \frac{\partial v_B}{\partial \theta_B} \Bigg\} \qquad \text{(A-4)}$$

4. TRANSFORMATION OF THE DERIVATIVE OF TEMPERATURE IN THE RADIAL DIRECTION

$$\frac{\partial T}{\partial r_s} = \left(\frac{\partial \theta_B}{\partial r_s}\right) \frac{\partial T}{\partial \theta_B} + \left(\frac{\partial r_B}{\partial r_s}\right) \frac{\partial T}{\partial r_B}$$

Thus,

$$\frac{\partial T}{\partial r_s} = \frac{[r_B + d \cos \theta_B]}{[r_B^2 + d^2 + 2dr_B \cos \theta_B]^{\frac{1}{2}}} \frac{\partial T}{\partial r_B}$$

$$- \frac{[d \sin \theta_B]}{[r_B^2 + d^2 + 2dr_B \cos \theta_B]^{\frac{1}{2}} r_B} \frac{\partial T}{\partial \theta_B} \qquad \text{(A-5)}$$

With Eqs. (A-1)-(A-5), the shock conservation Eqs. (I-6) in Section I can readily be expressed in the (r_B, θ_B) coordinate system as in the form of Eqs. (II-3).

APPENDIX B

COEFFICIENTS OF THE SHOCK CONSERVATION EQUATIONS (EQS. V-5)

In the following expressions for the coefficients, all the terms involve f and g and their derivatives are evaluated at $\eta = {}_0\eta_1$, and ${}_2y_1 = \frac{e}{2}\left(\frac{1+{}_0y_1}{1+{}_0y_1+e}\right)$

$$K_1 = \frac{1}{3\bar{\mu}_e}\left[2\,{}_0\eta_1\left(\frac{f'}{f}\right) - 1\right]$$

$$K_2 = \frac{1}{3\bar{\mu}_e}\left[2\,{}_0\eta_1\left(\frac{f'}{f}\right) - 1\right]$$

$$K_3 = 0$$

$$K_4 = \frac{f'}{f}$$

$$K_5 = \frac{(1+{}_0y_1)^2}{2(1+{}_0y_1+e)} - \left[\frac{{}_0\eta_1}{2}\left(\frac{f'}{f}\right) + \frac{1}{6}\right]$$

$$Y_1 = \frac{1}{3\bar{\mu}_e} - 1$$

$$Y_2 = \frac{1}{3\bar{\mu}_e} - 1$$

$$Y_3 = 0$$

$$Y_4 = \frac{g}{\int_0^{{}_0\eta_1} g\,d\eta}$$

$$Y_5 = \frac{1}{6} - \frac{1}{2\,{}_0y_1}\left[(1+{}_0y_1) - \frac{(1+{}_0y_1)^2}{(1+{}_0y_1+e)}\right]$$

$$\Theta_1 = \left\{f'\,{}_1\bar{u}_e(1+{}_0y_1+e)^2\right\} + \varepsilon_1\left\{\frac{e^2}{1+{}_0y_1}\left(\frac{4\,{}_0\eta_1\,g'}{3\,{}_0\bar{\rho}_e\bar{\mu}_e}\right)\right.$$

$$- (1+{}_0y_1+e)\left(\frac{e}{1+{}_0y_1}\right)\left[3f'\,{}_1\bar{u}_e + \frac{4}{3}\,\frac{f''\,{}_0\eta_1}{\bar{\mu}_e}\;{}_1\bar{u}_e\right]$$

$$- e(1+{}_0y_1+e)\left[\frac{4\,{}_0\eta_1 f''}{3\bar{\mu}_e}\;{}_1\bar{u}_e + 4f'\,{}_1\bar{u}_e + \frac{2fg'}{g}\left(1-\frac{1}{3\bar{\mu}_e}\right)\,{}_1\bar{u}_e\right]$$

$$\left. + 2ff''\,{}_1\bar{u}_e^2\,{}_0\bar{\rho}_e(1+{}_0y_1+e)^2\left(2-\frac{1}{3\bar{\mu}_e}\right)\right\}$$

$$\Theta_2 = \left\{\frac{eg}{{}_0\bar{\rho}_e}(1+{}_0y_1+e)\right\} + \varepsilon_1\left\{-\left(\frac{g}{{}_0\bar{\rho}_e}\right)\left(\frac{e}{1+{}_0y_1}\right)(1+{}_0y_1+e)\right.$$

$$+ \frac{e^2}{1+{}_0y_1}\left[\frac{4\,{}_0\eta_1\,g'}{3\,{}_0\bar{\rho}_e\,\bar{\mu}_e} - \frac{2g}{{}_0\bar{\rho}_e}\right] - \frac{4}{3}\,\frac{{}_1\bar{u}_e\,f''\,{}_0\eta_1}{\bar{\mu}_e}(1+{}_0y_1+e)\left(\frac{e}{1+{}_0y_1}\right)$$

$$- e(1+{}_0y_1+e)\left[\frac{4\,{}_0\eta_1\,f''}{3\bar{\mu}_e}\;{}_1\bar{u}_e + 2f'\,{}_1\bar{u}_e - \frac{2fg'}{g}\,\frac{{}_1\bar{u}_e}{3\bar{\mu}_e}\right]$$

$$\left. + 2ff''\,{}_1\bar{u}_e^2\,{}_0\bar{\rho}_e(1+{}_0y_1+e)^2\left(1-\frac{1}{3\bar{\mu}_e}\right)\right\}$$

$$\Theta_3 = 0$$

$$\Theta_4 = \left\{ - \left(\frac{eg'}{{}_0\bar{\rho}_e}\right) (1 + {}_0y_1 + e) + {}_1\bar{u}_e \, f'' (1 + {}_0y_1 + e)^2 \right\}$$

$$+ \varepsilon_1 \left\{ \left(\frac{g'}{{}_0\bar{\rho}_e}\right) \frac{e}{1 + {}_0y_1} (1 + {}_0y_1 + e) - (1 + {}_0y_1 + e) \left(\frac{e}{1 + {}_0y_1}\right) f'' \, {}_1\bar{u}_e \right.$$

$$- e(1 + {}_0y_1 + e) \left[2f'' \, {}_1\bar{u}_e + 2f \, {}_1\bar{u}_e \left(\frac{g''}{g} - \left(\frac{g'}{g}\right)^2\right)\right]$$

$$\left. + 2ff'' \, {}_1\bar{u}_e^2 \, {}_0\bar{\rho}_e (1 + {}_0y_1 + e)^2 \left(\frac{f'''}{f''}\right) \right\}$$

$$\Theta_5 = \left\{ \left(\frac{eg}{{}_0\bar{\rho}_e}\right) \left[-(2 + {}_0y_1) \left({}_2y_1 - \frac{1 + {}_0y_1}{2}\right) + \frac{1}{6} (1 + {}_0y_1 + e) + {}_2y_1 (1 + {}_0y_1)\right] \right.$$

$$+ ({}_1\bar{u}_e f') (1 + {}_0y_1 + e) \left(2 \, {}_2y_1 - \frac{1 + {}_0y_1}{2} - \frac{e}{2}\right)$$

$$\left. - \left[(1 + {}_0y_1 + e) \left({}_2y_1 - \frac{1 + {}_0y_1}{6}\right) + (1 + {}_0y_1) \left({}_2y_1 - \frac{1 + {}_0y_1}{2}\right)\right] \right\}$$

$$+ \varepsilon_1 \left\{ -\left(\frac{eg}{{}_0\bar{\rho}_e}\right) \left(\frac{1}{1 + {}_0y_1}\right) \left[\left(\frac{e}{1 + {}_0y_1}\right) {}_2y_1 + \frac{e}{2} + \frac{(1 + {}_0y_1)^2}{2} + \frac{1}{6} (1 + {}_0y_1 + e)\right] \right.$$

$$+ \frac{e^2 \, {}_1\bar{u}_e f'}{1 + {}_0y_1} + \left(\frac{e^2}{1 + {}_0y_1}\right) \left[\frac{{}_0\eta_1 \, g'}{3 \, {}_0\bar{\rho}_e} - \left(\frac{g}{{}_0\bar{\rho}_e}\right) \frac{(1 + {}_0y_1)^2}{(1 + {}_0y_1 + e)}\right]$$

$$\left. + ({}_1\bar{u}_e f') \left(\frac{e}{1 + {}_0y_1}\right) \left[\left(\frac{1}{6} + \frac{{}_2y_1}{1 + {}_0y_1}\right) (1 + {}_0y_1 + e) - \left({}_2y_1 - \frac{e}{2}\right)\right] \right.$$

$$- \left({}_1\bar{u}_e f' \right) e \left[{}_2y_1 - \frac{e}{2} - \frac{1}{6} \left(1 + {}_0y_1 + e \right) \right] \left[2 - \frac{2fg'}{f'g} \right]$$

$$+ \left({}_1\bar{u}_e f' \right) e \left(1 + {}_0y_1 + e \right) \left[\frac{1}{3} - \frac{1}{3} \, {}_0\eta_1 \, \frac{f''}{f'} + \frac{1}{3} \, \frac{fg'}{f'g} + \frac{\left(1 + {}_0y_1 \right)^2}{\left(1 + {}_0y_1 + e \right)} \, \frac{fg'}{f'g} \right]$$

$$+ \left[2ff'' \, {}_1\bar{u}_e^2 \, {}_0\bar{\rho}_e \right] \left[2 \left(1 + {}_0y_1 + e \right) \left({}_2y_1 - \frac{e}{2} \right) - \frac{1}{6} \left(1 + {}_0y_1 + e \right)^2 \right]$$

$$- \left(1 + {}_0y_1 + e \right) \left(\frac{e}{1 + {}_0y_1} \right) \left(\frac{1}{3} \, f'' \, {}_0\eta_1 \, {}_1\bar{u}_e \right) \Bigg\}$$

$$P_1 = \epsilon_2 \left\{ \left(1 + {}_0y_1 + e \right)^2 \left({}_1\bar{u}_e f' \right) \left[\frac{4 \, {}_0\eta_1 \, f''}{3\bar{\mu}_e \, f'} + 4 + \frac{2fg'}{f'g} \left(1 - \frac{1}{3\bar{\mu}_e} \right) \right] \right.$$

$$\left. - \left(\frac{g}{{}_0\bar{\rho}_e} \right) \frac{e}{1 + {}_0y_1} \left(1 + {}_0y_1 + e \right) \left(\frac{4 \, {}_0\eta_1 \, f'}{3g \, \bar{\mu}_e} \right) \right\}$$

$$P_2 = \left\{ \left(\frac{\Gamma - 1}{\Gamma} \right) {}_0\bar{\rho}_e \, {}_0\bar{h}_{se} \left(1 + e + {}_0y_1 \right)^2 - \left(\frac{\Gamma + 1}{2\Gamma} \right) \left(1 + e + {}_0y_1 \right)^2 \left(\frac{g}{{}_0\bar{\rho}_e} \right) \right\}$$

$$+ \epsilon_2 \left\{ \left(1 + e + {}_0y_1 \right)^2 \left({}_1\bar{u}_e f' \right) \left[\frac{4 \, {}_0\eta_1 \, f''}{3\bar{\mu}_e \, f'} + 2 - 2 \, \frac{fg'}{f'g} \, \frac{1}{3\bar{\mu}_e} \right] \right.$$

$$\left. + \left(\frac{g}{{}_0\bar{\rho}_e} \right) \frac{e}{1 + {}_0y_1} \left(1 + {}_0y_1 + e \right) \left[2 - \frac{4 \, {}_0\eta_1 \, g'}{3g \, \bar{\mu}_e} \right] \right\}$$

$$P_3 = \left(\frac{\Gamma - 1}{\Gamma} \right) {}_0\bar{\rho}_e \, {}_0\bar{h}_{se} \left(1 + e + {}_0y_1 \right)^2$$

$$P_4 = \left\{ \left(\frac{\Gamma+1}{2\Gamma}\right) (1+e+{}_0y_1)^2 \left(\frac{g'}{{}_0\bar{\rho}_e}\right) \right\}$$

$$+ \epsilon_2 \left\{ (1+{}_0y_1+e)^2 \, ({}_1\bar{u}_e f') \left[\frac{2f''}{f'} + \frac{2fg''}{f'g} - \frac{2f}{f'} \left(\frac{g'}{g}\right)^2\right] \right\}$$

$$P_5 = \Bigg[{}_0\bar{\rho}_e \; {}_0\bar{h}_{se} \left\{ \left(\frac{\Gamma-1}{\Gamma}\right) \left[2 \, {}_2y_1 \, (1+{}_0y_1) + 2e \left({}_2y_1 - \frac{1+{}_0y_1}{2}\right)\right] \right\}$$

$$+ \left(\frac{g}{{}_0\bar{\rho}_e}\right) \left\{ \left(\frac{\Gamma-1}{2\Gamma}\right) \left[-2 \, {}_2y_1 \, (1+{}_0y_1) - 2e \left({}_2y_1 - \frac{1+{}_0y_1}{2}\right) + (1+e+{}_0y_1)(1+{}_0y_1)^2\right] \right.$$

$$\left. + (1+{}_0y_1+e) \left[2 \, {}_2y_1 - \frac{1+{}_0y_1}{2} - \frac{e}{2} - \frac{1}{2} (1+{}_0y_1)^2\right] \right\}$$

$$- \left\{ \left(\frac{\Gamma-1}{2\Gamma}\right) \left(\frac{{}_0\bar{\rho}_e}{g}\right) ({}_1\bar{u}_e f')^2 (1+e+{}_0y_1)^2 \right\}$$

$$- \bar{p}_\infty \left\{ 2 \, {}_2y_1 \, (1+{}_0y_1) + 2e \left({}_2y_1 - \frac{1+{}_0y_1}{2}\right) \right\}$$

$$\left. + \left\{ (1+{}_0y_1+e) \, (1+{}_0y_1 - 2 \, {}_2y_1) \right\} + ({}_1\bar{u}_e f') \left\{ e(1+{}_0y_1+e) \right\} \right]$$

$$+ \epsilon_2 \left[\left(\frac{g}{{}_0\bar{\rho}_e}\right) \left\{ \frac{e^2}{1+{}_0y_1} + \left(\frac{e}{1+{}_0y_1}\right) (1+{}_0y_1+e) \left[\frac{(1+{}_0y_1)^2}{(1+{}_0y_1+e)} - \frac{{}_0\eta_1 g'}{3g}\right] \right\} \right.$$

$$+ ({}_1\bar{u}_e f') \left\{ -e + (1+{}_0y_1+e)^2 \left[- \frac{(1+{}_0y_1)^2}{(1+{}_0y_1+e)} \frac{fg'}{f'g} + \frac{1}{3} \, {}_0\eta_1 \frac{f''}{f'} - \frac{1}{3} - \frac{1}{3} \frac{fg'}{f'g} \right] \right.$$

$$\left. \left. + 4(1+{}_0y_1+e) \left({}_2y_1 - \frac{e}{2}\right) \left(1+\frac{fg'}{f'g}\right) \right\} + 2ff'' \, {}_1\bar{u}_e^2 \, {}_0\bar{\rho}_e \left\{ e(1+{}_0y_1+e) \right\} \right]$$

$$E_1 = E_2 = (1+e+{}_0y_1)\,(1-\frac{1}{3\bar{\mu}_e})\,[\bar{h}_{s\,\infty} - {}_0\bar{h}_{se}\,g] - \epsilon_2\,(\frac{e}{1+{}_0y_1})\,(\frac{4\,{}_0\bar{h}_{se}\,{}_0\eta_1\,g'}{3\bar{\mu}_e})$$

$$E_3 = (1+e+{}_0y_1)\,\bar{h}_{s\,\infty} - \epsilon_2\,(\frac{e}{1+{}_0y_1})\,(2g\,{}_0\bar{h}_{se})$$

$$E_4 = (1+e+{}_0y_1)\,\left\{[\frac{g''}{g'} - \frac{g'}{g}]\,(\bar{h}_{s\,\infty} - {}_0\bar{h}_{se}\,g) + {}_0\bar{h}_{se}\,g'\right\}$$

$$E_5 = (1+{}_0y_1+e)^{-1}\,[{}_0\bar{h}_{se}\,g - \bar{h}_{s\,\infty}]\,\left\{(5\,{}_2y_1 - \frac{1+{}_0y_1}{2})\,(1+{}_0y_1) + 5e\,({}_2y_1 - \frac{1+{}_0y_1}{2})\right.$$

$$\left. + (1+e+{}_0y_1)\,({}_2y_1 - \frac{e}{2})\right\} - \frac{1}{6}\,[1+{}_0y_1+e]\,[\bar{h}_{s\,\infty} - {}_0\bar{h}_{se}\,g]$$

$$+ \frac{\epsilon_2}{3}\,\left\{(\frac{g}{{}_0\bar{\rho}_e})^2\,[\frac{e^2}{1+{}_0y_1}\,(1+{}_0y_1+e)^{-1}] - (\frac{g}{{}_0\bar{\rho}_e})\,({}_1\bar{u}_e\,f')[(\frac{e^2}{1+{}_0y_1})\,(1+{}_0y_1+e)^{-1}\right.$$

$$\left. + 2e^2(1+{}_0y_1+e)^{-1} + (\frac{e}{1+{}_0y_1}) + 2e^2(1+{}_0y_1+e)^{-1}\,(\frac{fg'}{f'g})]\right.$$

$$+ ({}_1\bar{u}_e\,f')^2\,[(\frac{e}{1+{}_0y_1}) + 2e + 2e\,(\frac{fg}{f'g})] + (\frac{g}{{}_0\bar{\rho}_e})\,({}_1\bar{u}_e\,f')^2\,{}_0\bar{\rho}_e\,[2e\,\frac{ff''}{(f')^2}]$$

$$\left. - ({}_1\bar{u}_e\,f')^3\,{}_0\bar{\rho}_e\,[(1+{}_0y_1+e)\,\frac{2ff''}{(f')^2}] - [(\frac{e}{1+{}_0y_1})\,{}_0\bar{h}_{se}\,{}_0\eta_1\,g']\right\}$$

TABLE I

DENSITY AND STAGNATION ENTHALPY AS FUNCTIONS

OF THE MATCHING DISTANCE (BOUNDARY LAYER COORDINATE)

$_{o}\eta_{1}$	$_{o}\bar{\rho}_{e}$	$_{o}\bar{\rho}_{1}$	$_{2}\bar{\rho}_{e}/_{o}\bar{\rho}_{e}$	$_{o}\bar{h}_{se}$	$_{o}\bar{h}_{s1}$	$_{2}\bar{h}_{se}/_{o}\bar{h}_{se}$
1.09673	11.05477	22.01497	-13.4165	0.20894	0.10492	-4.7526
1.21880	10.07088	18.21337	- 4.6405	0.24876	0.13755	-2.4403
1.34087	9.19259	15.27922	- 1.8802	0.28847	0.17355	-0.4414
1.46293	8.49328	13.10819	- 1.2757	0.32697	0.21185	-0.1217
1.58501	7.94828	11.49356	- 0.9753	0.36338	0.25129	-0.0103
1.70708	7.52670	10.27952	- 0.7736	0.39697	0.29066	-0.0008
1.82915	7.20195	9.35658	- 0.6604	0.42730	0.32890	-0.0000
1.95122	6.95294	8.64844	- 0.5503	0.45410	0.36508	-0.0000
2.07329	6.76294	8.10105	- 0.4351	0.47735	0.39850	-0.0000
2.19536	6.62178	7.67899	- 0.3831	0.49716	0.42871	-0.0000
2.31743	6.51633	7.35049	- 0.3512	0.51377	0.45546	-0.0000
2.43950	6.44005	7.09629	- 0.2800	0.52748	0.47870	-0.0000

TABLE II

REYNOLDS NUMBER VERSUS $_{o}\eta_{1}$, $_{o}y_{1}$, e, $_{1}\bar{u}_{e}$, and $\dot{q}/\dot{q}_{B.L.}$

$_{o}\eta_{1}$	$_{o}y_{1}$	e	$_{1}\bar{u}_{e}$	ϵ	Re_{s}	$\dot{q}/\dot{q}_{B.L.}$
1.09673	0.0572	0.0640	0.6388	0.0376	18	0.664
1.21880	0.0600	0.0555	0.6685	0.0338	20	0.738
1.34087	0.0627	0.0472	0.7005	0.0286	24	0.798
1.46293	0.0648	0.0390	0.7343	0.0232	29	0.856
1.58501	0.0662	0.0316	0.7682	0.0183	37	0.911
1.70708	0.0669	0.0251	0.8026	0.0148	46	0.964
1.82915	0.0673	0.0197	0.8337	0.0100	61	1.011
1.95122	0.0675	0.0160	0.8607	0.0081	83	1.052
2.07329	0.0679	0.0135	0.8801	0.0061	110	1.089
2.19536	0.0683	0.0122	0.8931	0.0047	151	1.118
2.31743	0.0689	0.0120	0.8994	0.0033	203	1.143
2.43950	0.0694	0.0119	0.9043	0.0018	380	1.170

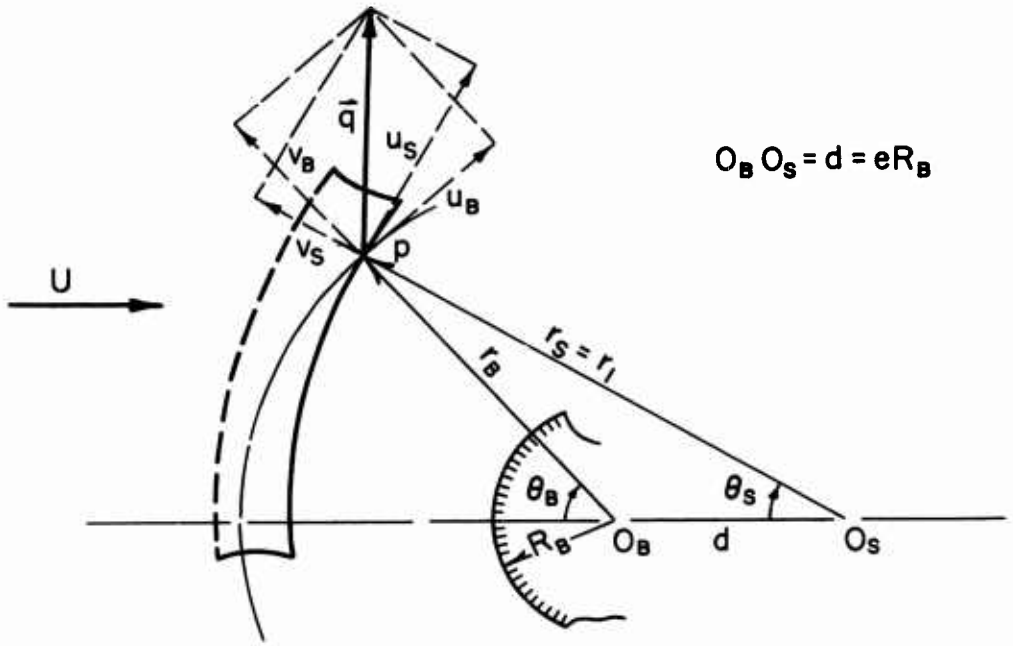

FIG. 1. Diagrammatical Drawing of the Shock and the Body

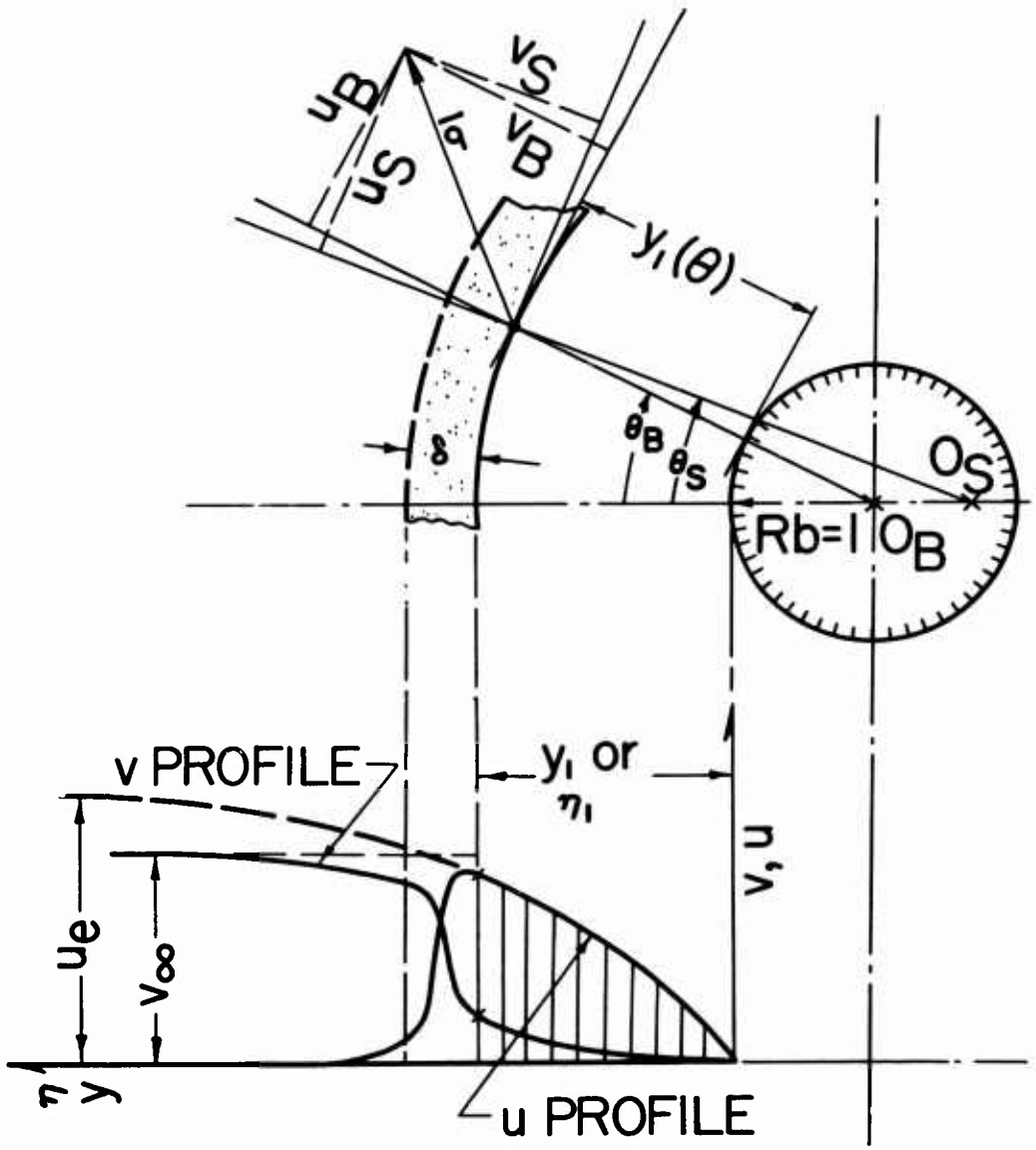

FIG. 2. Diagrammatical Drawing of the Matching Velocity Profiles

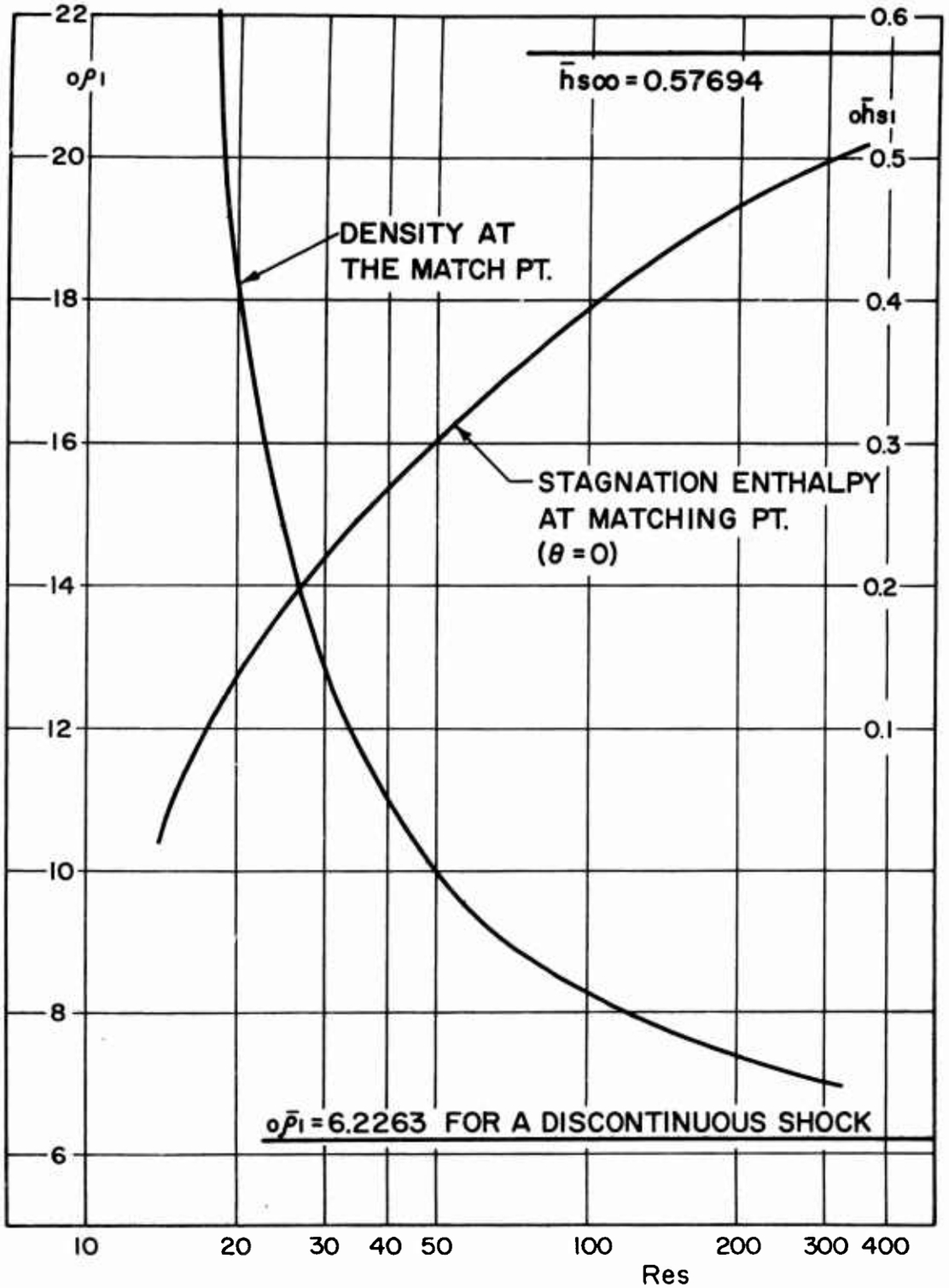

FIG. 3. Density and Stagnation Enthalpy at the Matching Point

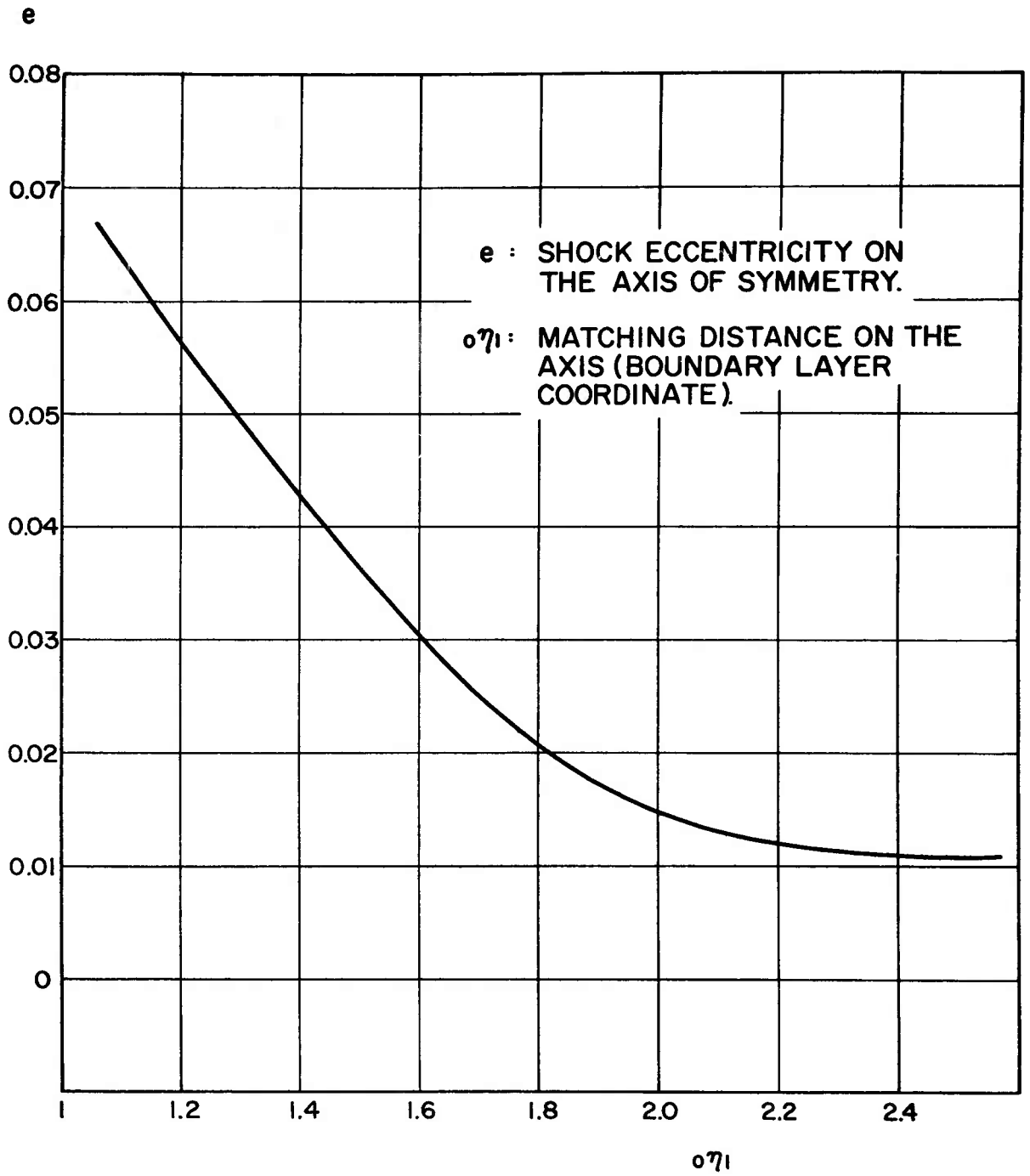

FIG. 4. The Eccentricity of the Matching Surface

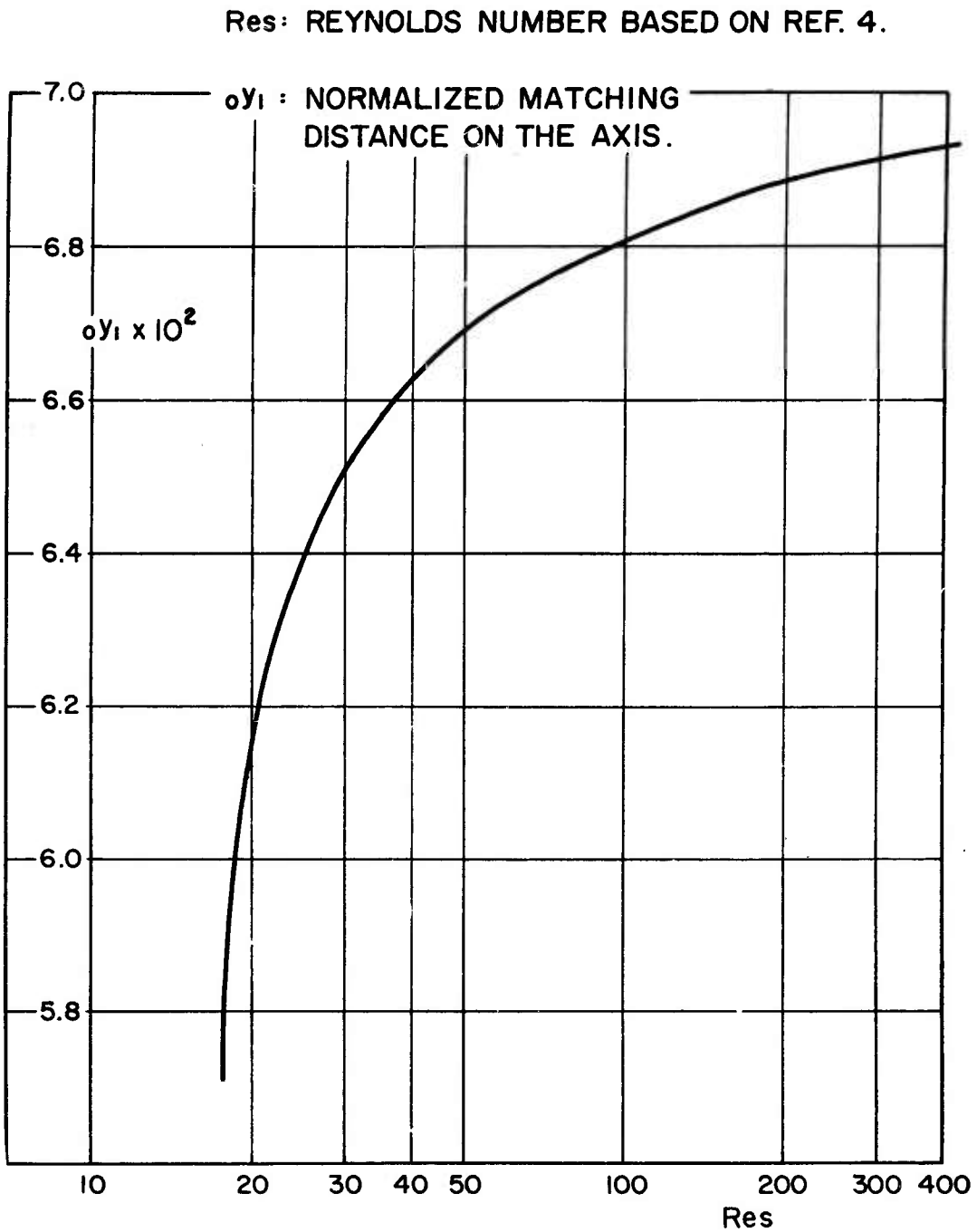

FIG. 5. Matching Distance on the Axis

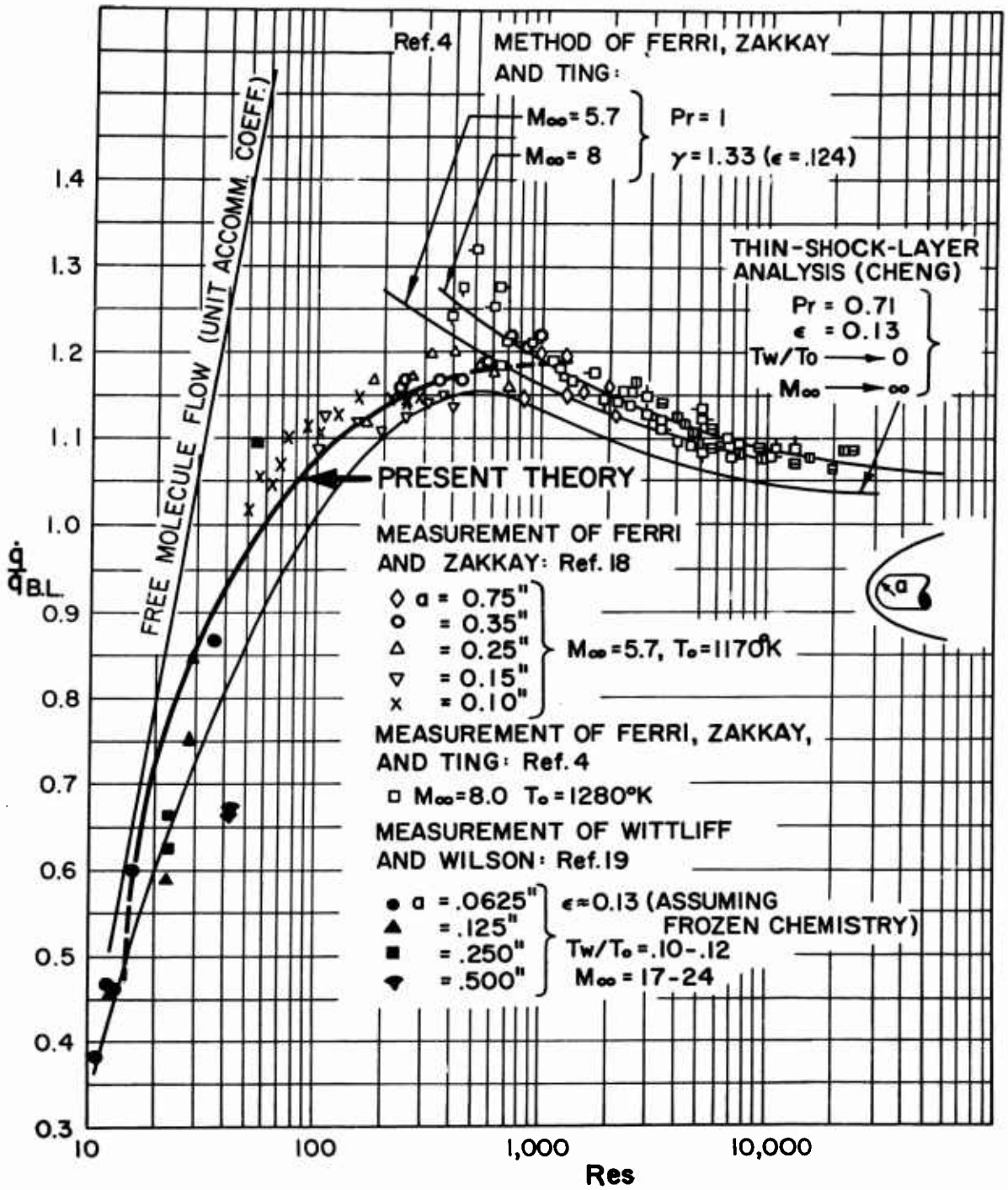

FIG. 6. Comparison of Stagnation Point Heat Transfer Measurements With Theories

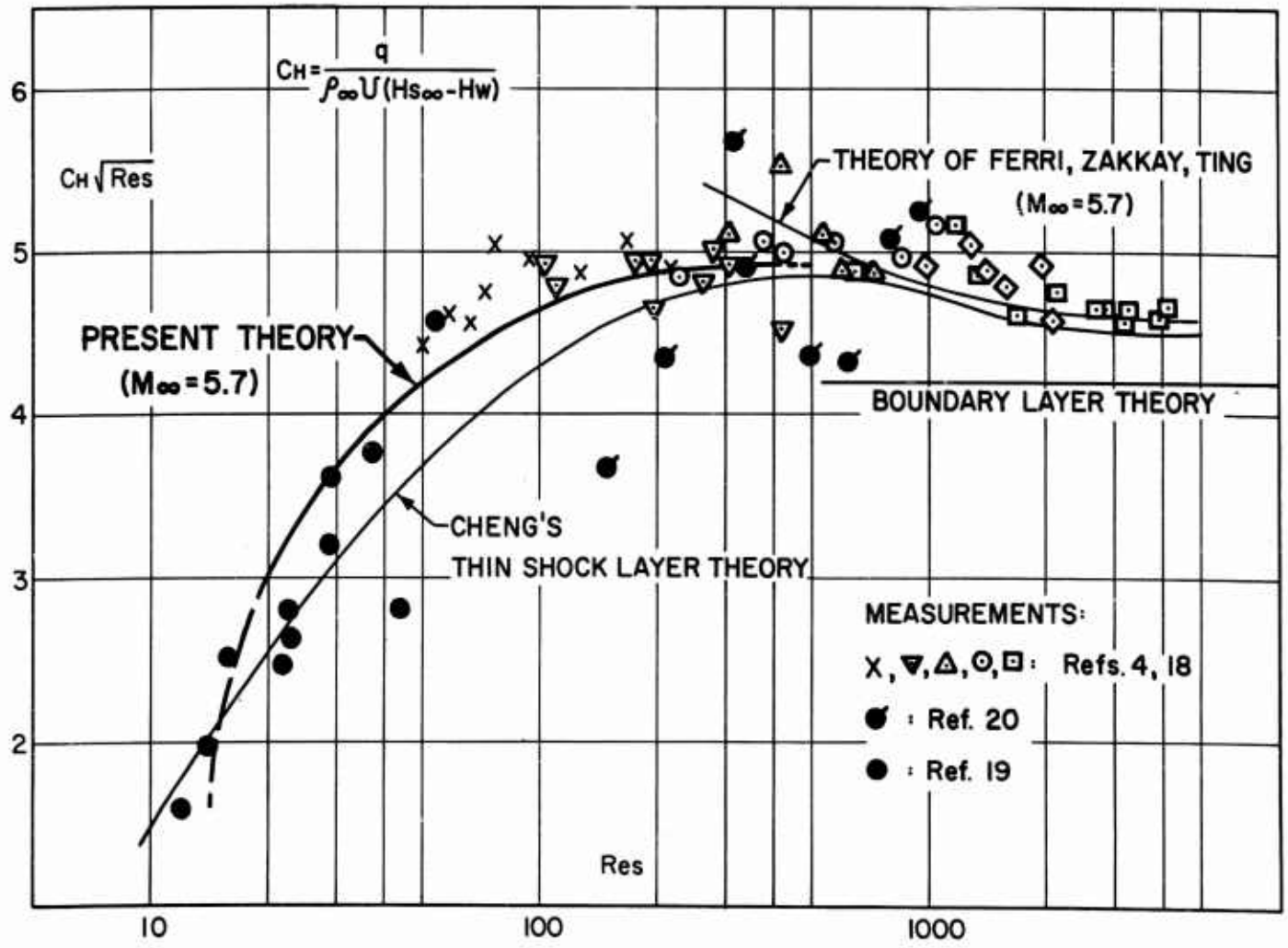

FIG. 7. Heat Transfer Value $C_H\sqrt{Re_s}$ Versus Re_s

Aeronautical Research Laboratories, Wright-Patterson AFB, O. HIGH SPEED LOW DENSITY FLOW NEAR THE STAGNATION POINT OF A BLUNT BODY by Rueben Ru-ren Chow, PIB, Brooklyn, N. Y. May 1963. 49 p. incl. illus. (Project 7064; Task 7064-01) (Contract AF 33(616)-7661) (ARL 63075)

Unclassified Report

The analysis is concerned with the investigation of the flow field near the stagnation point of a blunt body in a high speed low density stream. The leading order shock conditions are obtained from the systematic order of magnitude analysis. A matching scheme for the components of heat flux and stresses between the shock and the boundary layer has been proposed for the flow field study. A method of solution has been introduced so that the laborious job of numerical integration of the flow equations with complicated boundary conditions can be bypassed. Calculation has been performed for M_∞=5.7 and T_0=free stream stagnation temperature = 2100°R. Numerical results are presented for the surface heat transfer value, the matching distance, the density and the stagnation enthalpy at the matching surface as functions of the Reynolds number.

(over)

UNCLASSIFIED

1. Hypersonic Aerodynamics
2. Heat Transfer
3. Low Density Flow

I. Reuben Ru-ren Chow
II. Aeronautical Research Laboratories
III. Contract AF 33(616)-7661

UNCLASSIFIED

Aeronautical Research Laboratories, Wright-Patterson AFB, O. HIGH SPEED LOW DENSITY FLOW NEAR THE STAGNATION POINT OF A BLUNT BODY by Rueben Ru-ren Chow, PIB, Brooklyn, N. Y. May 1963. 49 p. incl. illus. (Project 7064; Task 7064-01) (Contract AF 33(616)-7661) (ARL 63075)

Unclassified Report

The analysis is concerned with the investigation of the flow field near the stagnation point of a blunt body in a high speed low density stream. The leading order shock conditions are obtained from the systematic order of magnitude analysis. A matching scheme for the components of heat flux and stresses between the shock and the boundary layer has been proposed for the flow field study. A method of solution has been introduced so that the laborious job of numerical integration of the flow equations with complicated boundary conditions can be bypassed. Calculation has been performed for M_∞=5.7 and T_0=free stream stagnation temperature = 2100°R. Numerical results are presented for the surface heat transfer value, the matching distance, the density and the stagnation enthalpy at the matching surface as functions of the Reynolds number.

(over)

UNCLASSIFIED

1. Hypersonic Aerodynamics
2. Heat Transfer
3. Low Density Flow

I. Reuben Ru-ren Chow
II. Aeronautical Research Laboratories
III. Contract AF 33(616)-7661

UNCLASSIFIED

Aeronautical Research Laboratories, Wright-Patterson AFB, O. HIGH SPEED LOW DENSITY FLOW NEAR THE STAGNATION POINT OF A BLUNT BODY by Rueben Ru-ren Chow, PIB, Brooklyn, N. Y. May 1963. 49 p. incl. illus. (Project 7064; Task 7064-01) (Contract AF 33(616)-7661) (ARL 63075)

Unclassified Report

The analysis is concerned with the investigation of the flow field near the stagnation point of a blunt body in a high speed low density stream. The leading order shock conditions are obtained from the systematic order of magnitude analysis. A matching scheme for the components of heat flux and stresses between the shock and the boundary layer has been proposed for the flow field study. A method of solution has been introduced so that the laborious job of numerical integration of the flow equations with complicated boundary conditions can be bypassed. Calculation has been performed for M_∞=5.7 and T_0=free stream stagnation temperature = 2100°R. Numerical results are presented for the surface heat transfer value, the matching distance, the density and the stagnation enthalpy at the matching surface as functions of the Reynolds number.

(over)

UNCLASSIFIED

1. Hypersonic Aerodynamics
2. Heat Transfer
3. Low Density Flow

I. Reuben Ru-ren Chow
II. Aeronautical Research Laboratories
III. Contract AF 33(616)-7661

UNCLASSIFIED

Aeronautical Research Laboratories, Wright-Patterson AFB, O. HIGH SPEED LOW DENSITY FLOW NEAR THE STAGNATION POINT OF A BLUNT BODY by Rueben Ru-ren Chow, PIB, Brooklyn, N. Y. May 1963. 49 p. incl. illus. (Project 7064; Task 7064-01) (Contract AF 33(616)-7661) (ARL 63075)

Unclassified Report

The analysis is concerned with the investigation of the flow field near the stagnation point of a blunt body in a high speed low density stream. The leading order shock conditions are obtained from the systematic order of magnitude analysis. A matching scheme for the components of heat flux and stresses between the shock and the boundary layer has been proposed for the flow field study. A method of solution has been introduced so that the laborious job of numerical integration of the flow equations with complicated boundary conditions can be bypassed. Calculation has been performed for M_∞=5.7 and T_0=free stream stagnation temperature = 2100°R. Numerical results are presented for the surface heat transfer value, the matching distance, the density and the stagnation enthalpy at the matching surface as functions of the Reynolds number.

(over)

UNCLASSIFIED

1. Hypersonic Aerodynamics
2. Heat Transfer
3. Low Density Flow

I. Reuben Ru-ren Chow
II. Aeronautical Research Laboratories
III. Contract AF 33(616)-7661

UNCLASSIFIED

UNCLASSIFIED